Structural and thermal evolution of the eastern Aar Massif basement and its sedimentary cover (Engelbergertal, Reusstal, Färnigen Zone near Susten Pass)

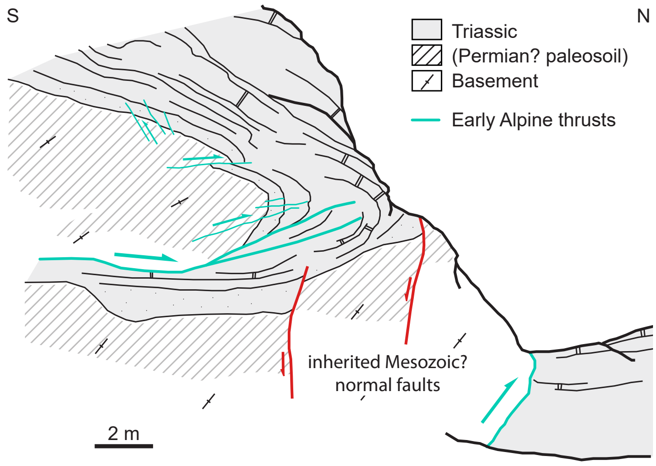

27.-29. August 2021

Lead: Lukas Nibourel[1,2], Marco Herwegh[2], Alfons Berger[2]

[1] Georesources Switzerland Group, Department of Earth Sciences, ETH Zürich
[2] Institute of Geological Sciences, University of Bern

Program

Day 1:
- Meeting point is 10 AM at Engelberg train station
- Main focus: thrusts at the external massif front, timing peak metamorphism and deformation
- One day hike at Engelbergertal

Day 2:
- Kinematic link to Subalpine Molasse and Helvetic nappes
- N-S-change of the overall structural appearance along the Reusstal transect
- Metamorphic evolution and exhumation of the massif
- Several stations by bus, transfer to the Susten Pass and overview Färnigen Zone

Day 3:
- Färnigen Zone, inherited normal faults and Alpine inversion,
- Overprinting relationships, different deformation behaviour of different lithostratigraphic units
- Stratigraphic affiliation?
- One day hike Färnigen Zone, Chli Griessenhorn

Under the following map link, you can find the approximate excursion program (click the link or scan the qr code below to access the map): https://s.geo.admin.ch/92ad84c943

General geologic-tectonic introduction

Tectonic overview: - Tectonic units
- Aar Massif formation mostly post-dates Helvetic nappe emplacement
- Kinematic link to Subalpine Molasse, Jura mountains
- Top basement -> orogen-scale marker
- Axial plunge of eastern Aar Massif

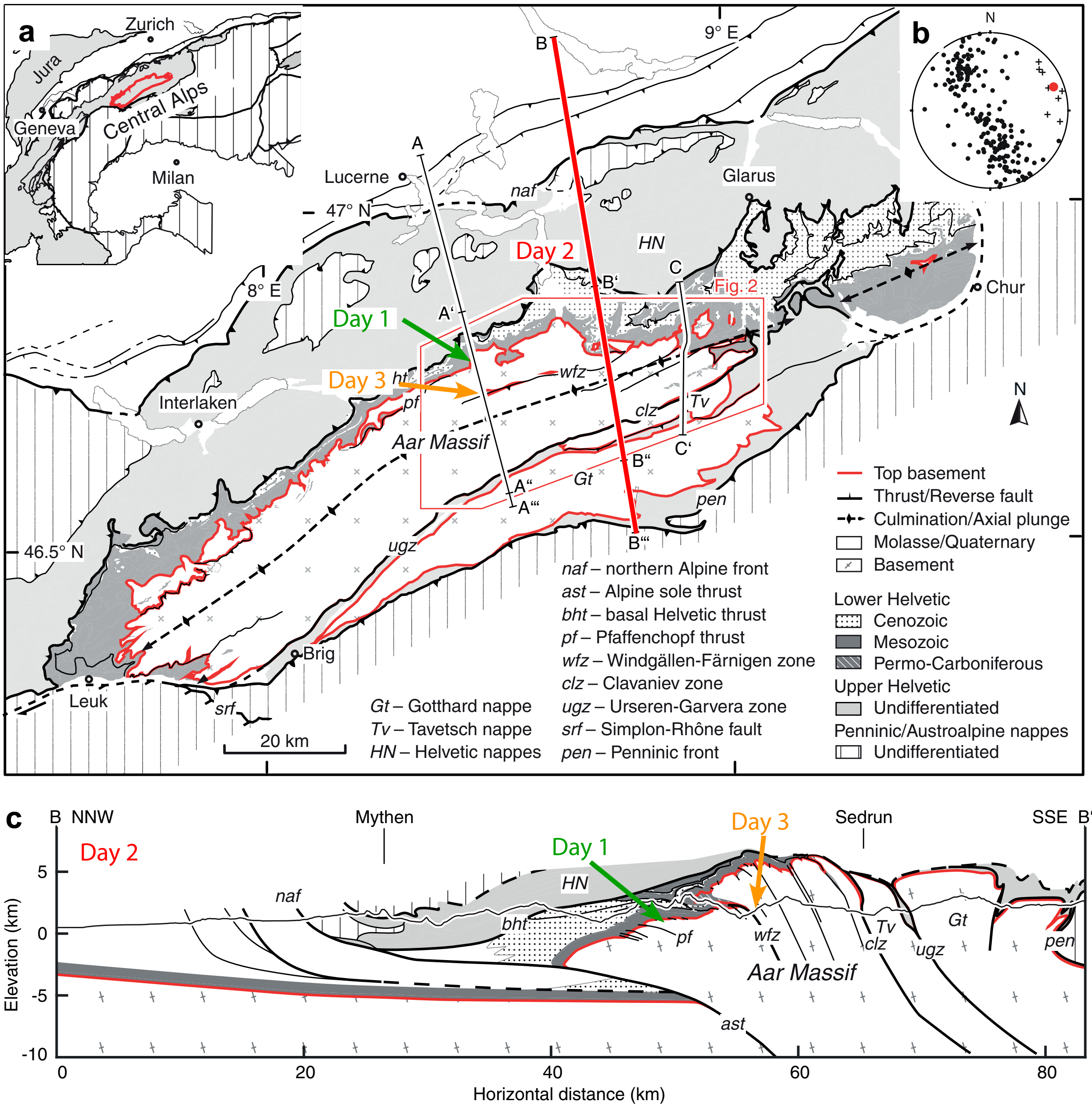

Fig. I-1: (a) Simplified tectonic map of the Aar Massif (modified after Schmid et al. 2004). Traces of cross sections A–A''' (Susten pass), cross sections B–B''' (Reusstal), cross section C–C' (Tödi) and the study area (red polygon) are highlighted. Inset modified after Schmid et al. (2004). (b) Stereographic projection shows poles to bedding (black dots, 227 measurements) and axes to early folds (black crosses, 8 measurements) from the sedimentary cover of the eastern Aar Massif (Schmidt, lower hemisphere). (c) Cross section B–B''' (in part after Brückner and Zbinden 1987; Pfiffner et al. 2011). See Nibourel et al., 2021 for details.

Alpine Metamorphic pattern: - Sub-greenschist to greenschist facies
- Reflects dome shape of the massif
- Timing deformation and peak metamorphism

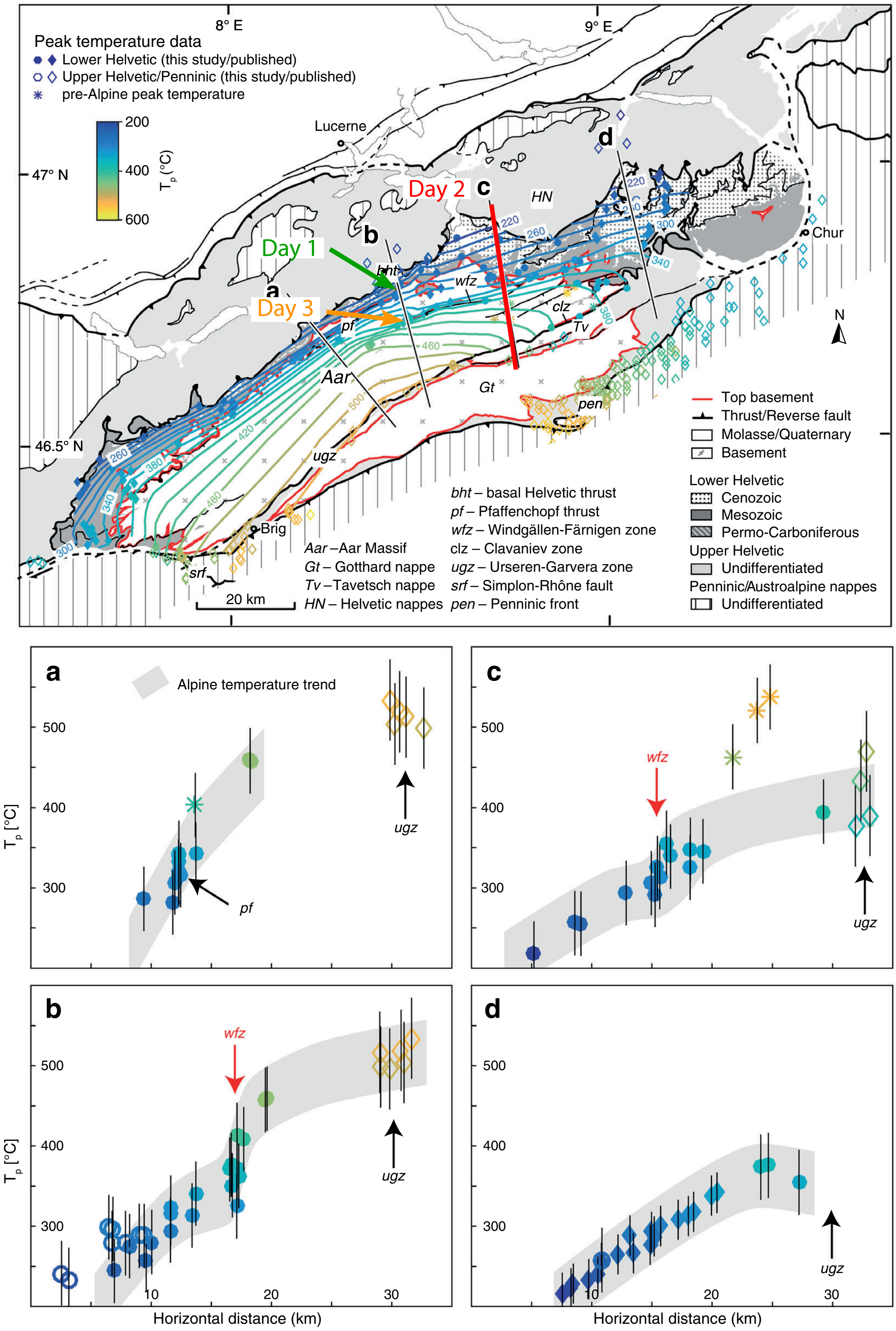

Fig. I-2: Simplified structural map (modified from Schmid et al. 2004) including new and published peak temperature estimates based on RSCM (Beyssac et al. 2002; Erne 2014; Girault et al. 2020; Hafner 2016; Lahfid et al. 2010; Mair et al. 2018; Negro et al. 2013; Nibourel et al. 2018; Wiederkehr et al. 2008) and calcite-dolomite thermometry data (Herwegh and Pfiffner 2005). See Nibourel et al. (2021) for details.

Geologic overview: - Mapped fault zones
- Polycyclic metamorphic basement and late-Variscan intrusives
- Mesozoic-Cenozoic cover sediments
- Local occurrences of Permo-Carboniferous sediments

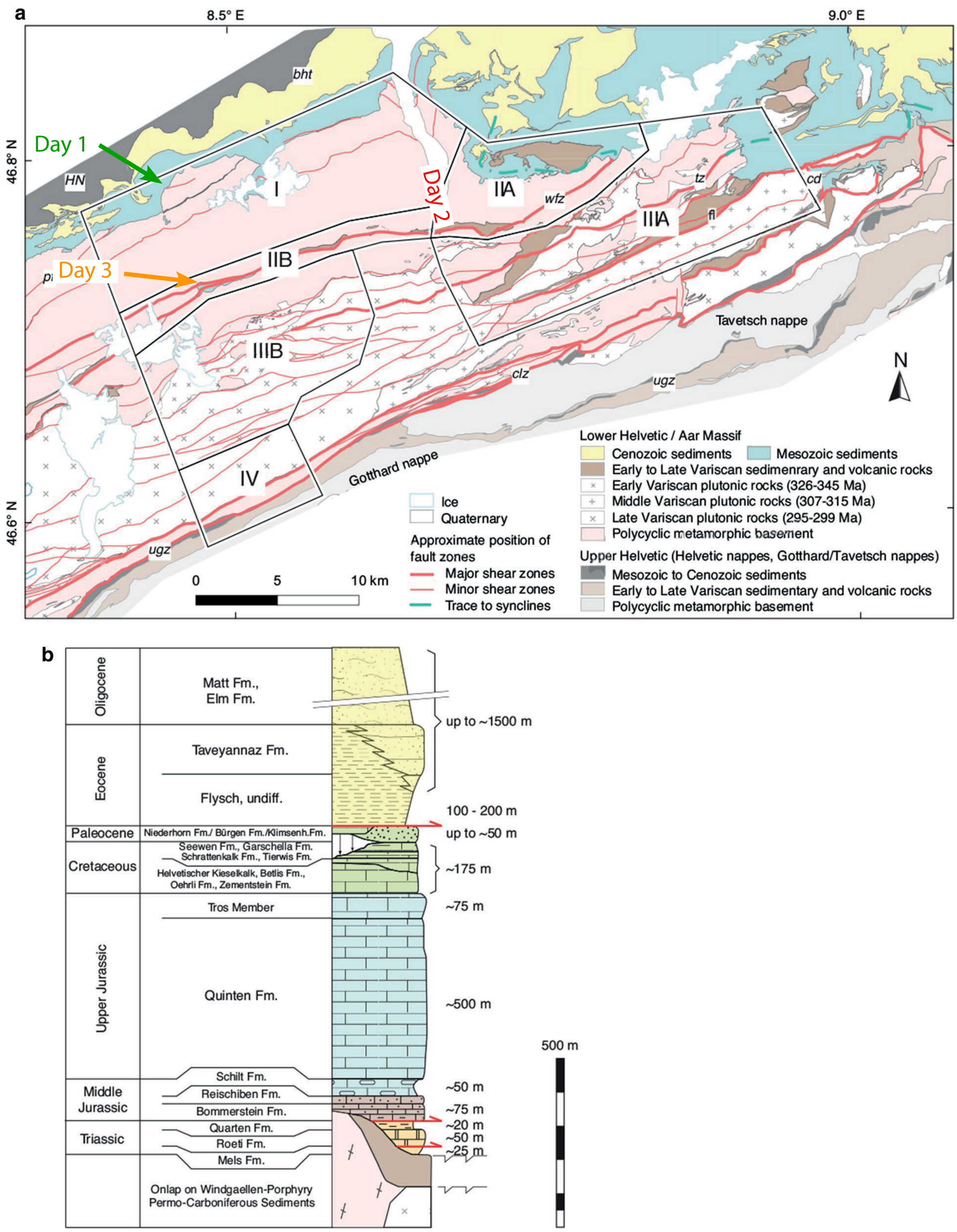

Fig. I-3: (a) Geological map of the Aar Massif (Nibourel et al., 2021) showing the simplified pattern of major (thickness > 20 m) and minor (2–20 m) Alpine basement shear zones and associated synclines in the cover units (partly modified from Baumberger 2015; Pfiffner 1978). HN—Helvetic nappes; bht—basal Helvetic thrust; pf—Pfaffenchopf thrust; wfz—Windgällen-Färnigen zone; tz—Tödi zone; fl—Frisal line; cd—Cavestrau décollement; clz—Clavaniev zone; ugz—Urseren-Garvera zone. (b) Summarised stratigraphic column of the eastern Aar Massif (modified after Gautschi et al. 2008; Pfiffner 2015).

Day 1, Overview

Topics: - Early and late thrusts at the northen Aar Massif
- Alpine D1 to D4 structures, pre-Alpine structures?
- Deformation in basement and cover units at T < 300 °C

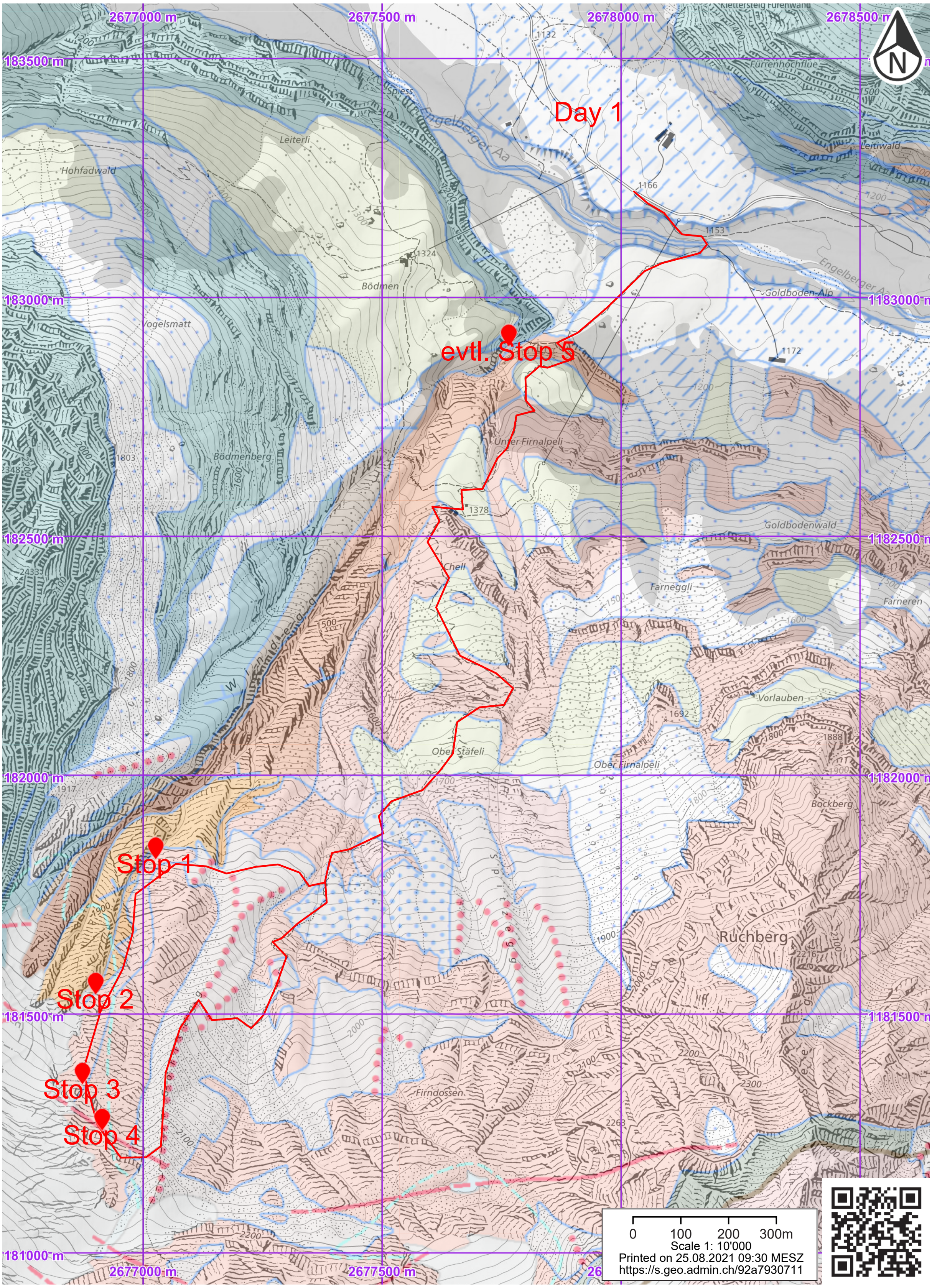

Fig. 1-1: Map overview of the most important stops in the Engelberg region.

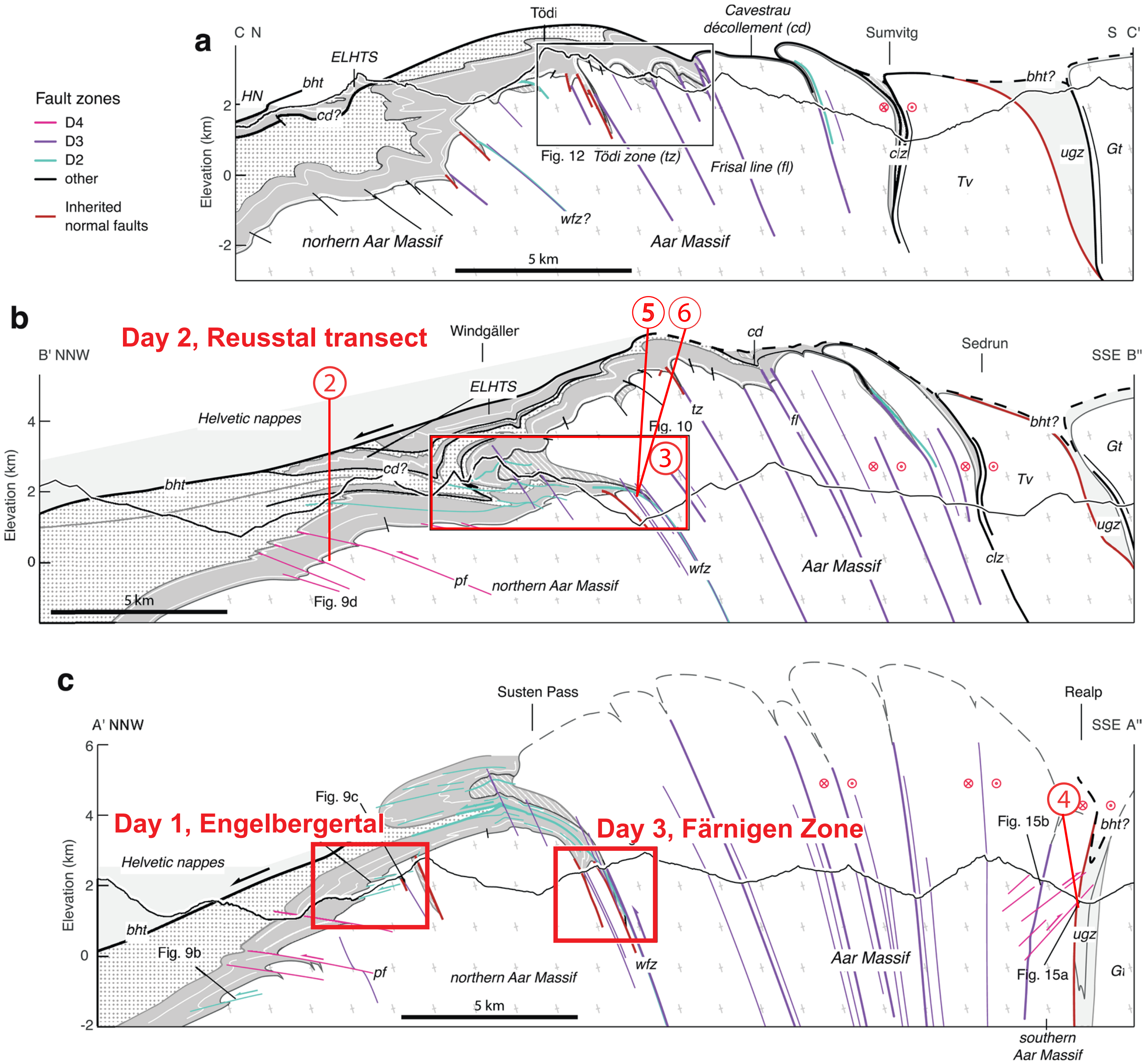

Fig. 1-2: Three stacked cross sections A-A'', B'-B'' and C-C' through the eastern Aar Massif. Section traces are shown on Fig. I-1. ELHTS — Early Lower Helvetic thrust sheets. Legend and abbreviations as in Fig. I-1. The approximate positions of Excursion days 1, 2 and 3 are highlighted as red rectangle (Fig. I-1).

Day 1, Stop 1

Topics:
- "Early" thrusts and relationship to inherited normal faults
- Passive northward tilting?
- Orientation top basement during D2?
- Timing peak metamorphism and deformation?
- No major detachment between basement and cover

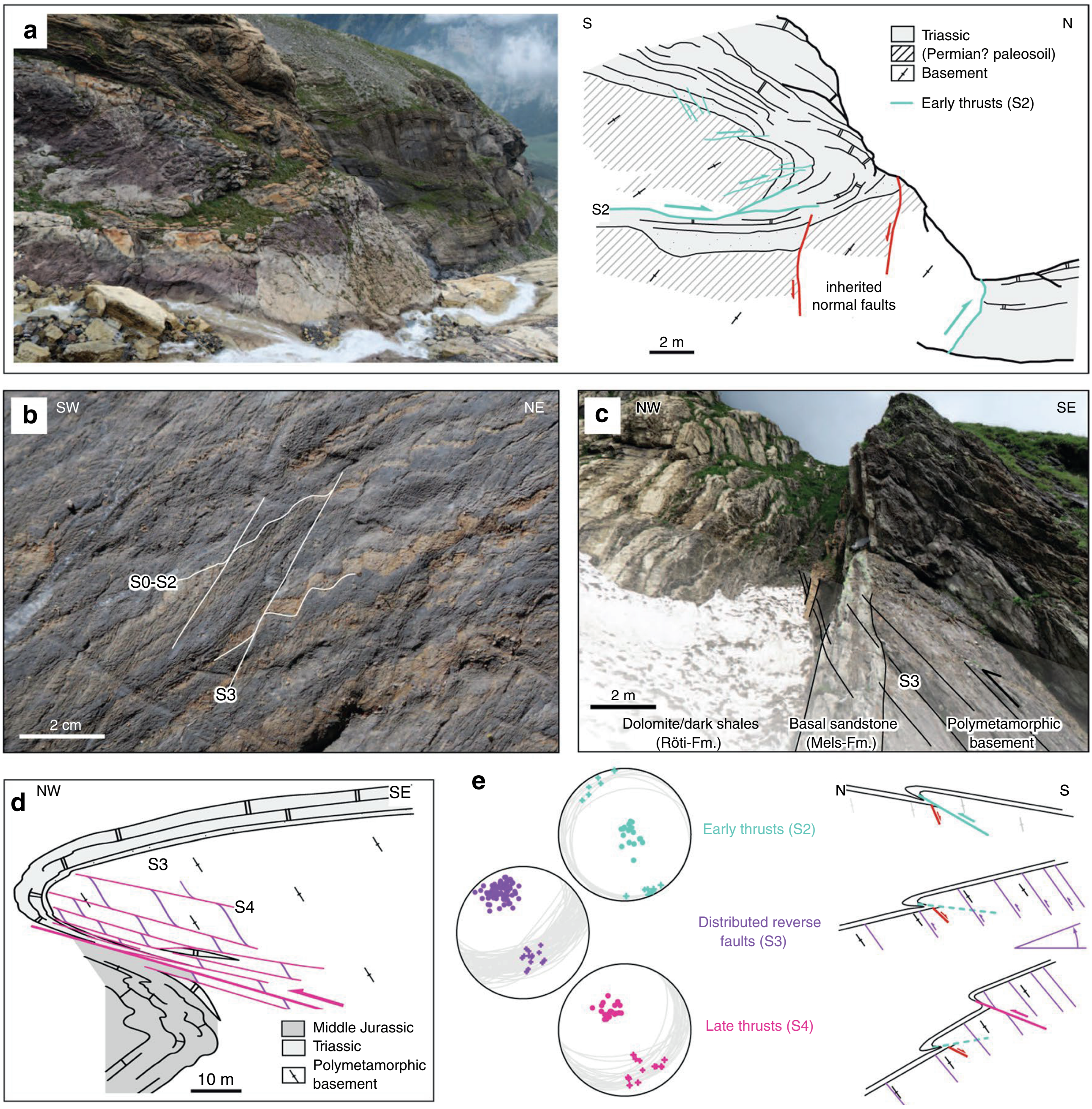

Fig. 1-3: (a) Early N-dipping NNW-vergent thrust (S2, coordinates: 46.7833°N/8.4474°E). (b) Steep SE-dipping spaced crenulation cleavage S3 in the Middle Jurassic limestones, overprinting a pronounced S0–S2 composite foliation (coordinates: 46.6523°N/8.1714°E). (c) Steep main foliation (S3) in both Triassic marly beds (left) and their crystalline substratum (right). The sub-vertical orientation of the stratigraphic contact indicates significant SSE-block up movements along S3 (coordinates: 46.7587°N/8.4027°E).(d) Sketch of an array of post-S3 NNW-vergent thrusts (S4) at the basement-cover interface near Erstfeld (coordinates: 46.8409°N/8.6264°E). (e) (left) Structural measurements related to NNW-vergent shearing during D2–D4. Poles to fault planes (circles) and associated stretching lineations (crosses) are highlighted. (right) Schematic sketch illustrating the geometric relationship between S2 and S4 at the basement-cover contact during progressive deformation and block rotation associated with S3 at the northern massif front. See Nibourel et al. (2021) for details.

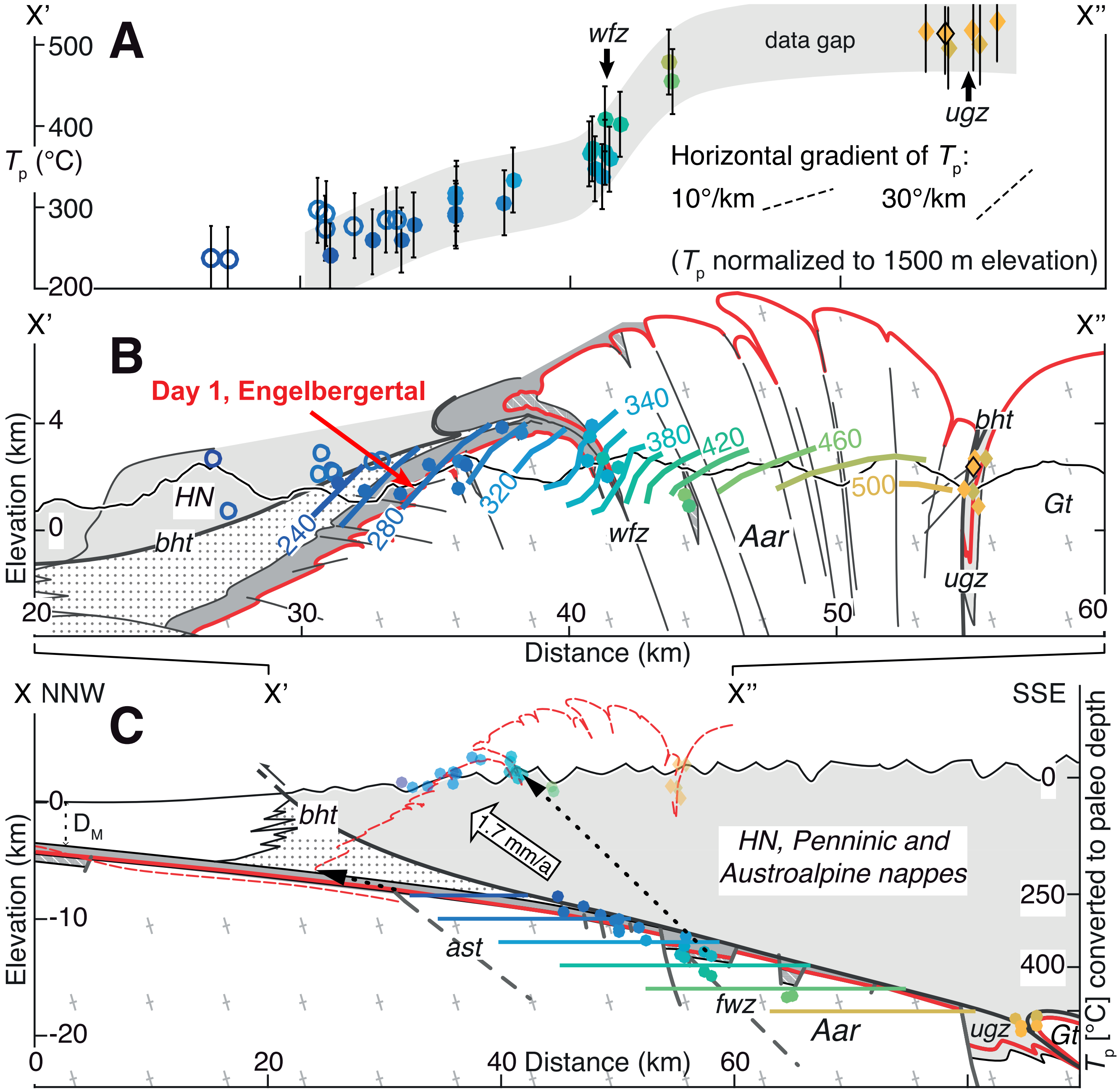

Fig. 1-4: (A) Evolution of metamorphic peak temperature (Tp) along the Susten Pass transect X'-X" in the eastern Aar Massif. (B) Tp plotted into cross section and isotherms. (C) Retro-deformed profile sketch of cross section X-X" prior to deformation at ca. 20 Ma. Top basement orientation and depth are based on Tp converted to depth (plain circles). DM—thickness of Lower Freshwater Molasse (Pfiffner, 2017). Present day positions of top basement (dashed red line) and samples (transparent circles) are shown for reference. Displacement vectors (dotted black vectors) and the average annual displacement over the past ~20 m.y. (southern Aar Massif, white arrow) are highlighted. Legend and abbreviations as in Fig. I-1. See Nibourel et al. (2018) for details.

Day 1, Stop 2

Topics:
- "Early" thrusts, direct observation in basement and dolomitic to marly cover units
- Discrete brittle-ductile faults in basement
- Discussion D1-D5 structures

Fig. 1-5: Strongly deformed marl and dolomite near the synclinal area to an "early" D2 thrust/fold (coordinates: 46.78087°N, 8.44582°E).

Day 1, Stop 3

Topics:
- Polycyclic metamorphic basement
- Alpine and pre-Alpine deformation?
- Discrete brittle-ductile faults in basement (Alpine?)
- No pervasive steep S3 as observed south of the Windgällen-Färnigen zone

Fig. 1-6: Contact between a basic enclave and the Innertkirchen Migmatite is offset by a brittle fault of unknown age (coordinates: 46.77891°N, 8.44521°E).

Day 1, Stop 4

Topics:
- Late-Alpine brittle fault
- Tight anticline in the calcite-dominated Schilt-Fm/Quinten-Fm

Fig. 1-7: Tight fold in the Jurassic strata of the Titlis east face (coordinates: 46.77804°N, 8.44576°E).

Day 2, Overview

Topics:
- Kinematic link to Subalpine Molasse and Helvetic nappes
- Metamorphic overprint and exhumation dynamics
- N-S transect, increasing metamorphic grade and structural appearence
- Windgällen fault-and-fold structure
- Overview Färnigen Zone

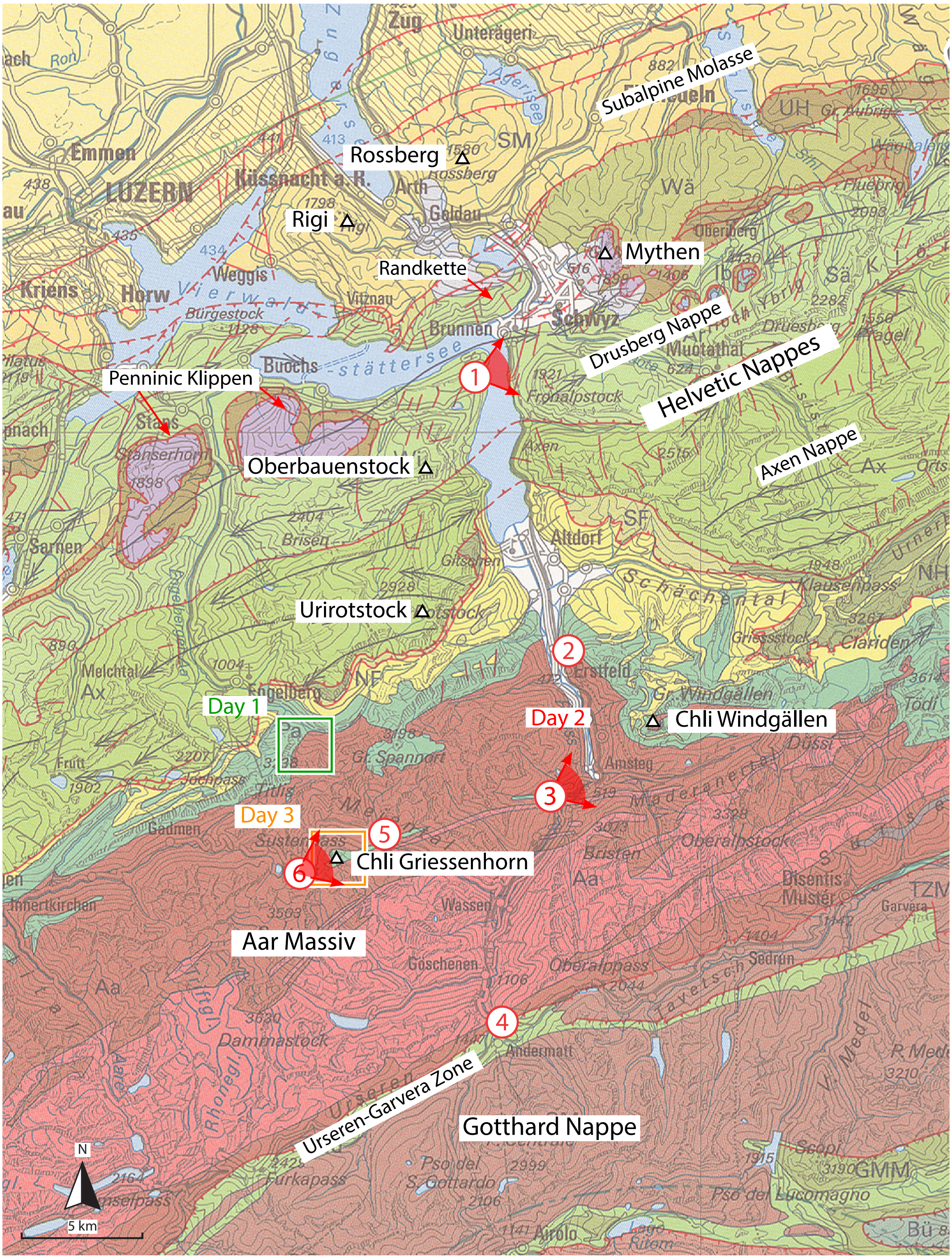

Fig. 2-1: Tectonic overview of the Reuss Valley area (Tectonic map of Switzerland, swisstopo).

Day 2, Stop 1 (Seelisberg)

Topics: - Kinematic link to Subalpine Molasse and Helvetic Nappes
- Root zone of the Helvetic nappes?

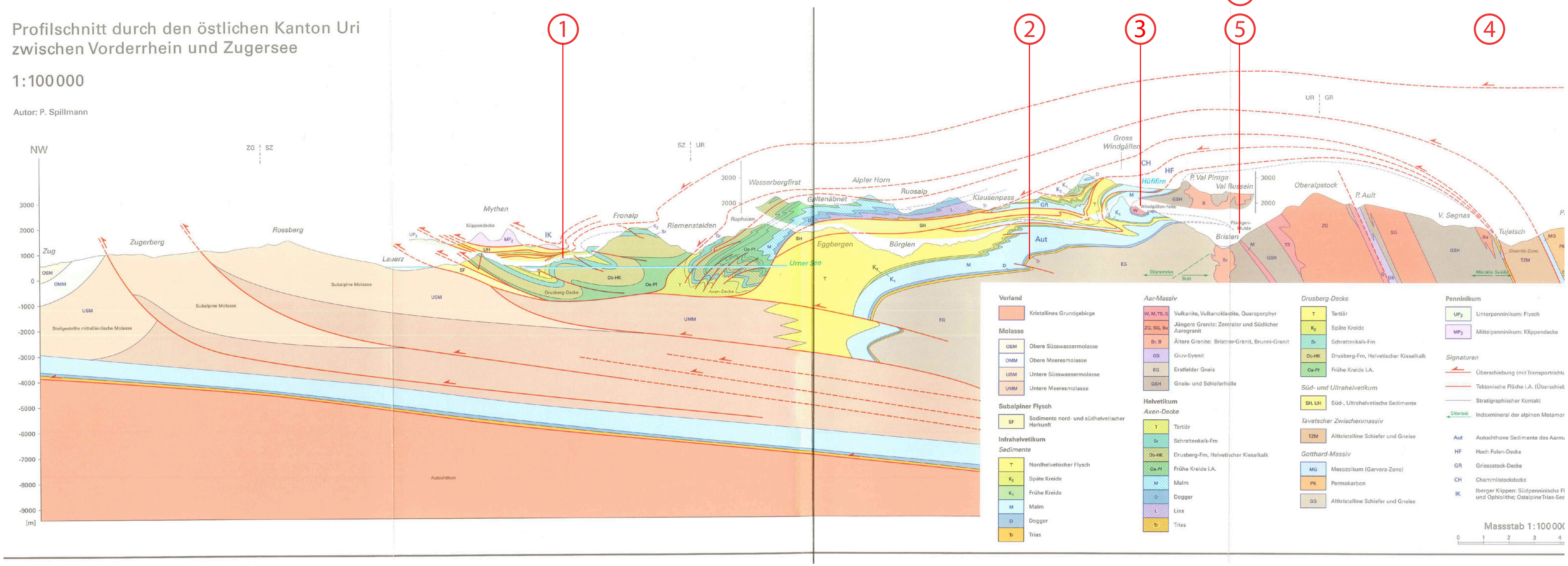

Fig. 2-2: Tectonic NW-SE cross-section along the eastern shore line of Lake Uri (Spillmann et al. 2011).

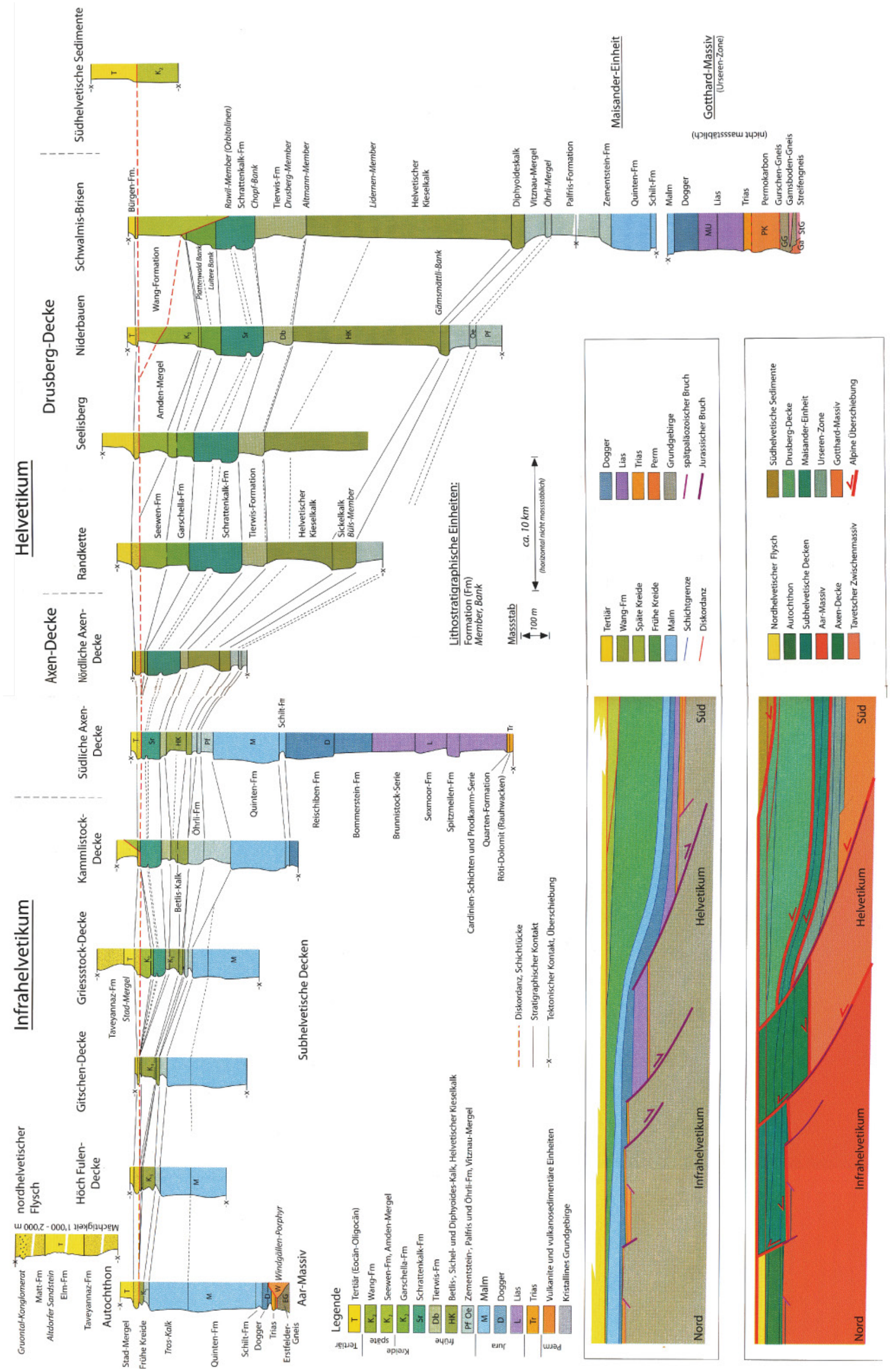

Fig. 2-3: Changes in thicknesses of Mesozoic sediments in a reconstructed N-S section. Lower two insets represent reconstructions of the European passive continental margin as well as the future thrust planes (Spillmann et al. 2011)

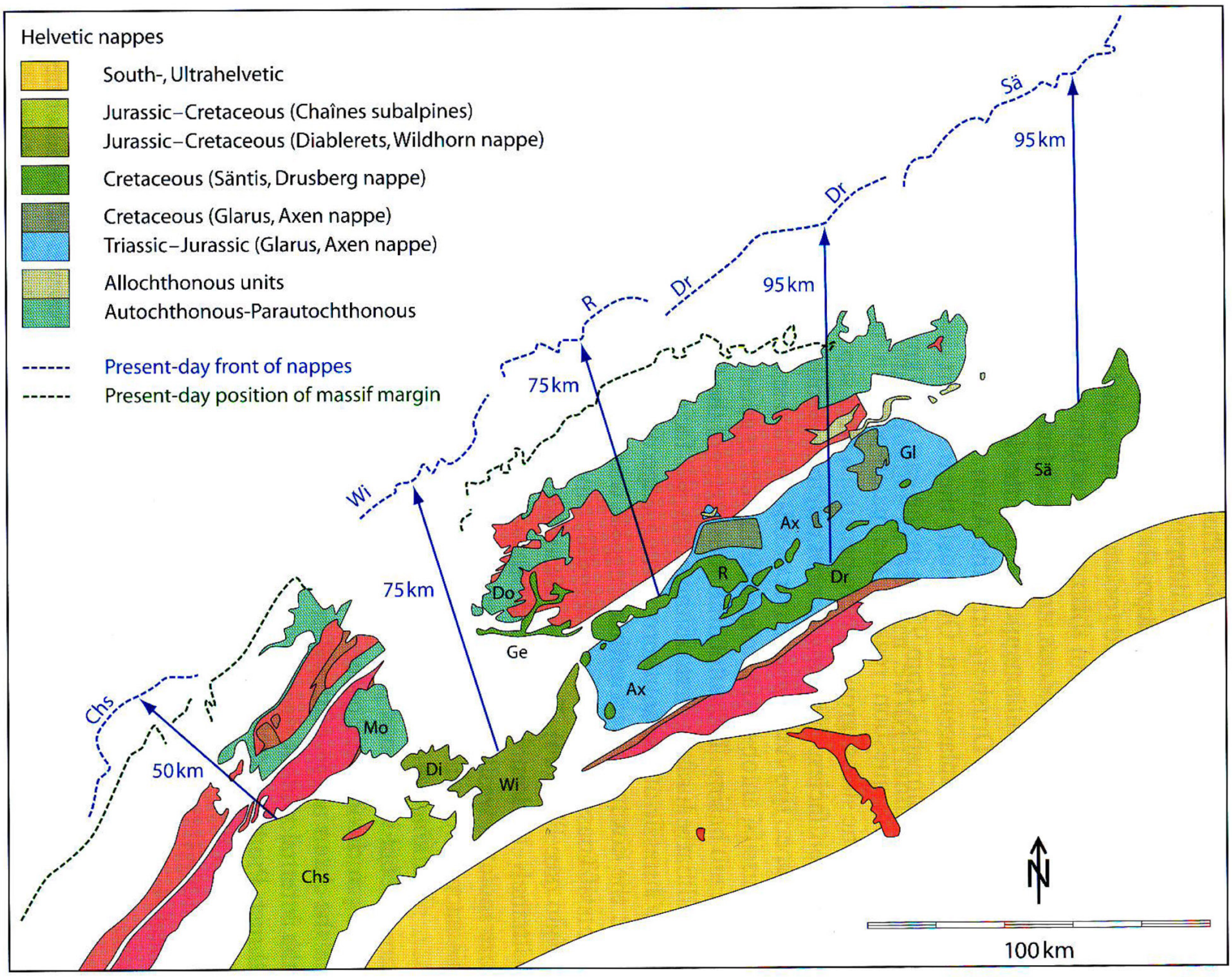

Fig. 2-4: Palinspastic reconstruction of the former locations of the External Crystalline Massifs as well as the Helvetic nappes (Pfiffner et al. 2011).

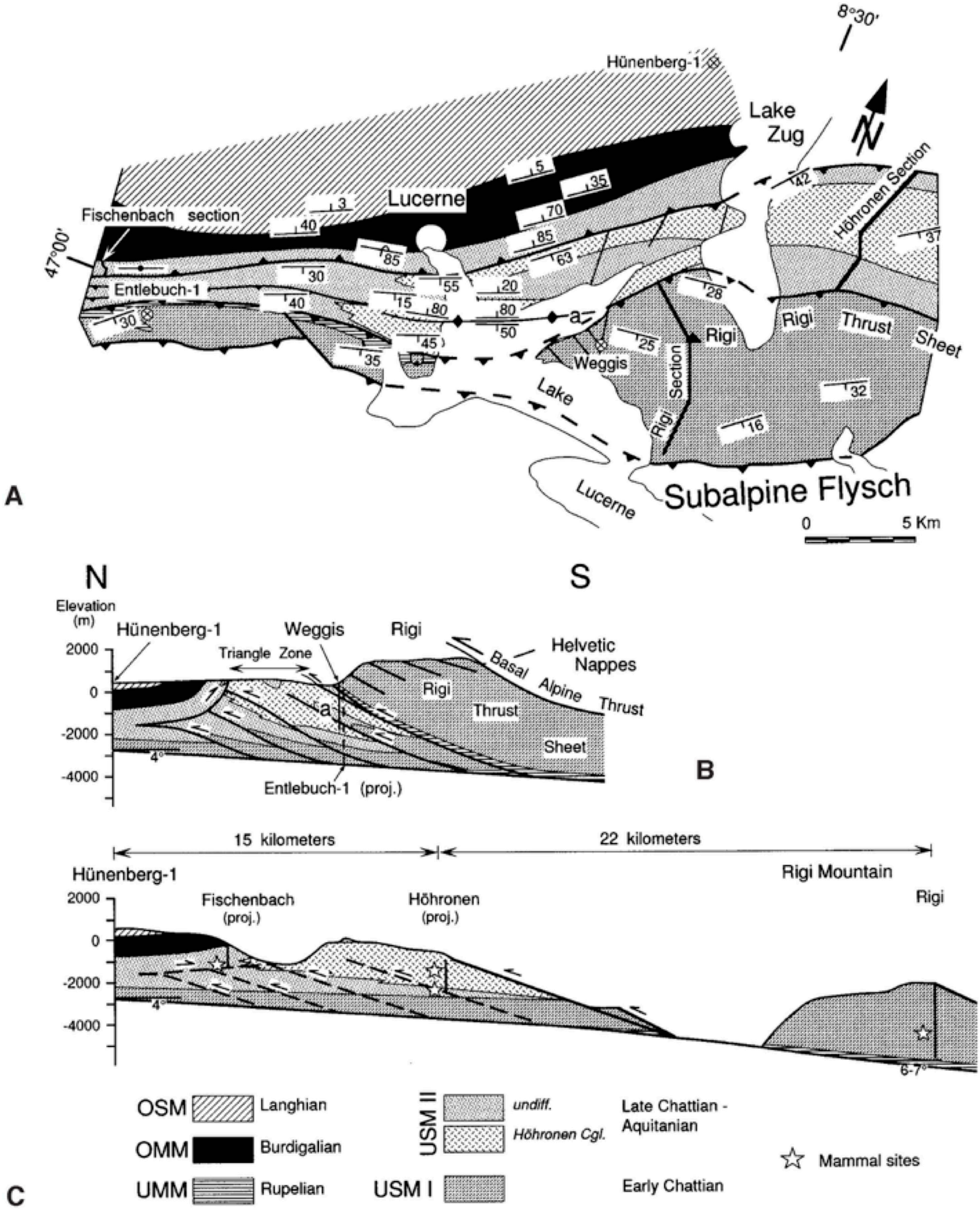

Fig. 2-5: The central Swiss Molasse basin with (A) a geologic map, (B) a cross section and (C) a palinspastic restoration (from Schlunegger et al. 1997).

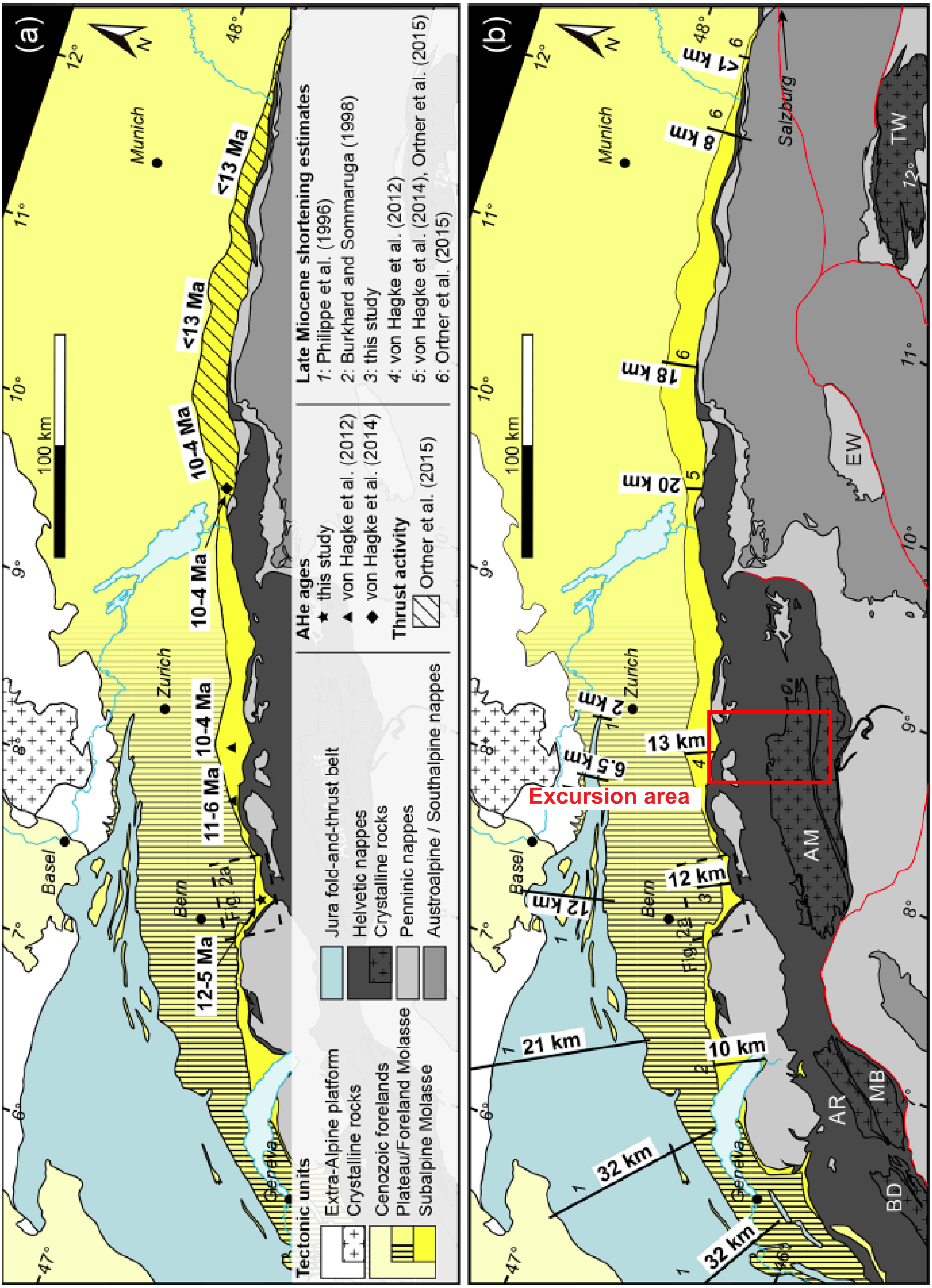

Fig. 2-6: Tectonic map of the Northalpine Foreland basin as well as age constraints of thrusting along the Subalpine Molasse (top) as well as estimated shortenings in the Subalpine Molasse and the Jura mountains (for details see Mock et al. 2020).

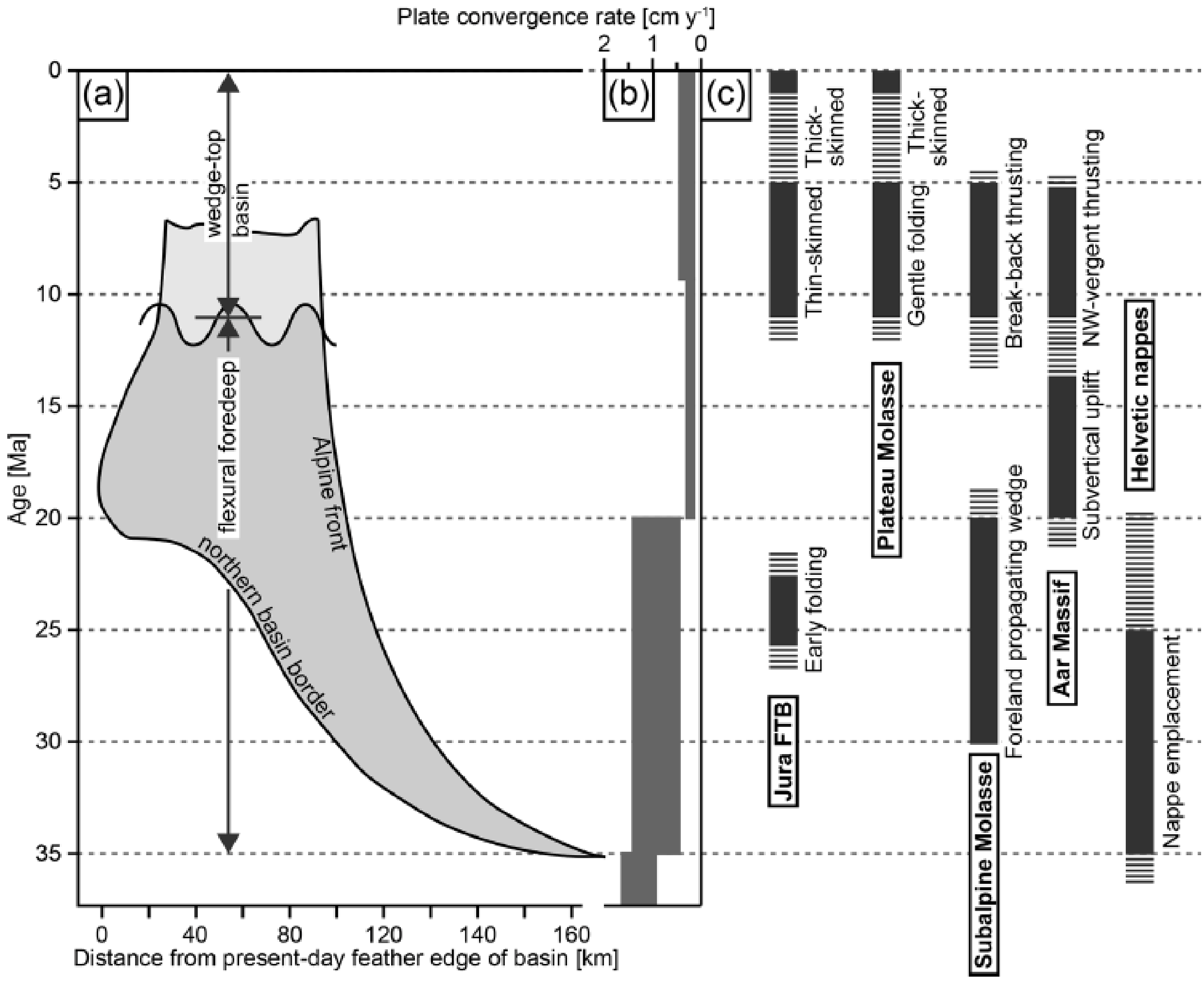

Fig. 2-7: Timetable and spatial progression of Northalpine front as well as northern border of the Molasse basin (for details see Mock et al. 2020).

Day 2, Stop 2

Topics:
- Basement-cover contact
- Pre-Alpine foliation
- "Late" D4 thrusts

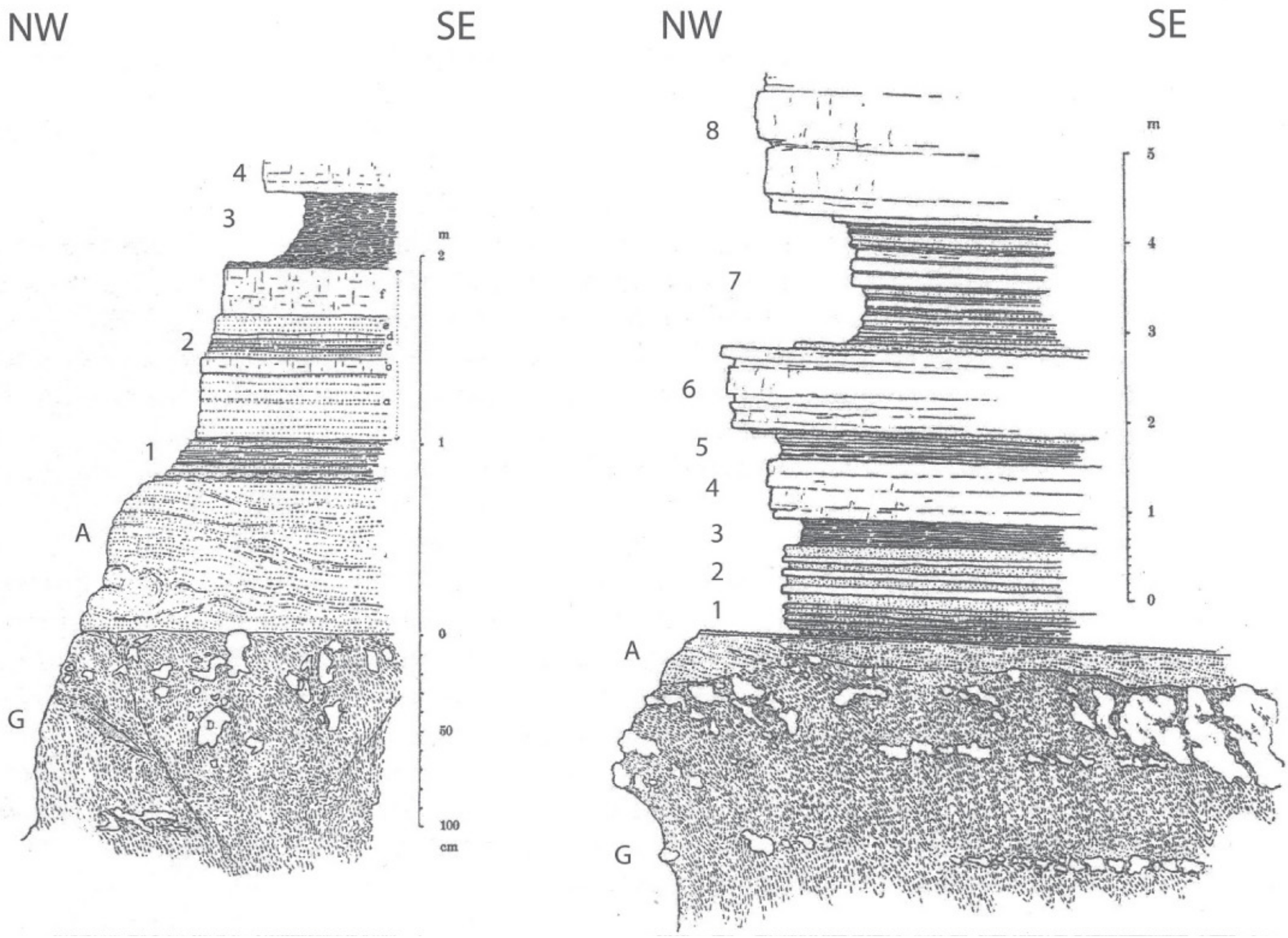

1) sandstone, slate
2) sandstone/dolomite
3) slate with sandy layers
4) layerd dolomite (65cm)
5) dolomite/slate
6) dolomite with wavy layers (90cm)
7) sand-clay interaclations with dolomite layers (1.5m)
8) dolomite (14-15m)

A) arkose
G) Erstfeld gneis

Fig. 2-8: Stratigraphic columns at Scheidnössli (Heim 1917, Coordinates: 46.83415°N, 8.64913°E).

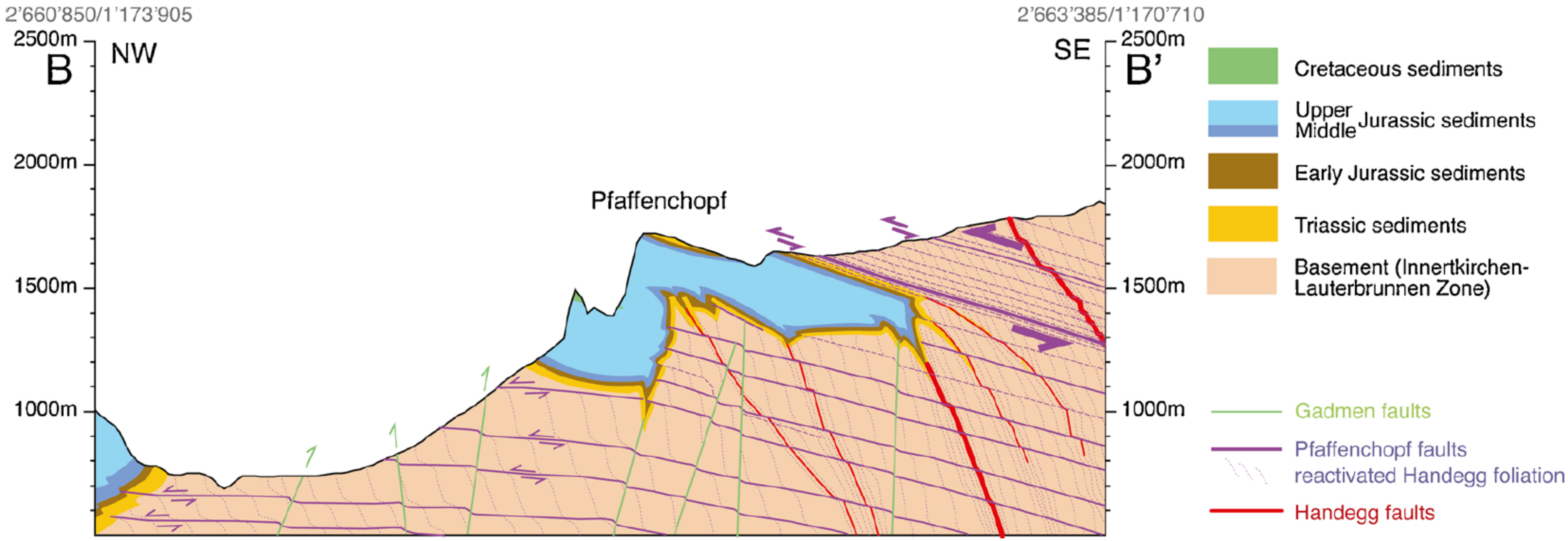

Fig. 2-9: The Pfaffenchopf thrust, the most prominent exposed D4 thrust of the Aar Massif (Herwegh et al., 2020). Note multiple deformational overprint and reactivation of pre-existing mechanical discontinuities by Handegg, Pfaffenchopf (array 1), and Gadmen faults.

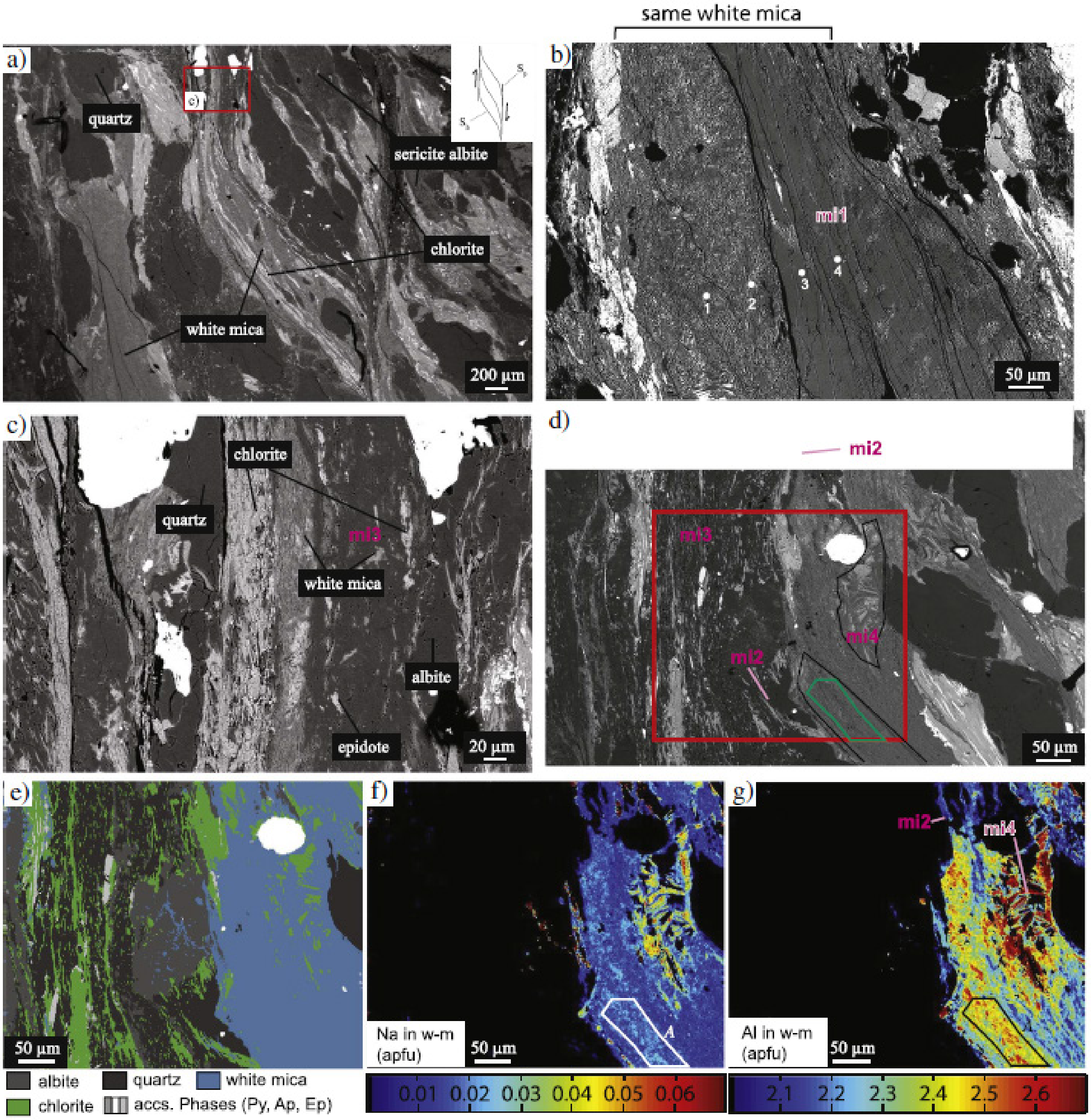

Fig. 2-10: Low temperature (< 300°C) deformation structures in the basement at the thin section scale. See Berger et al. (2017) for details.

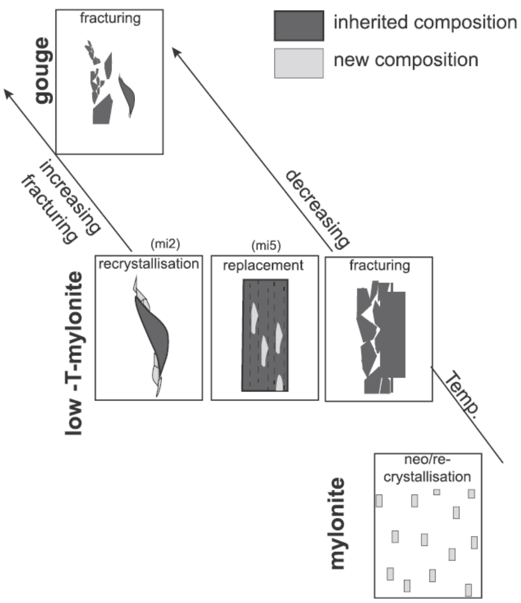

Fig. 2-11: Schematic sketch of low temperature (< 300°C) deformation mechanisms in the basement. See Berger et al. (2017) for details.

Day 2, Stop 3 Obergurtnellen

Topics:
- Steep pervasive foliation (S3) south of Windgällen-Färnigen zone
- Pre-D3 Windgällen fold-and-fault structure

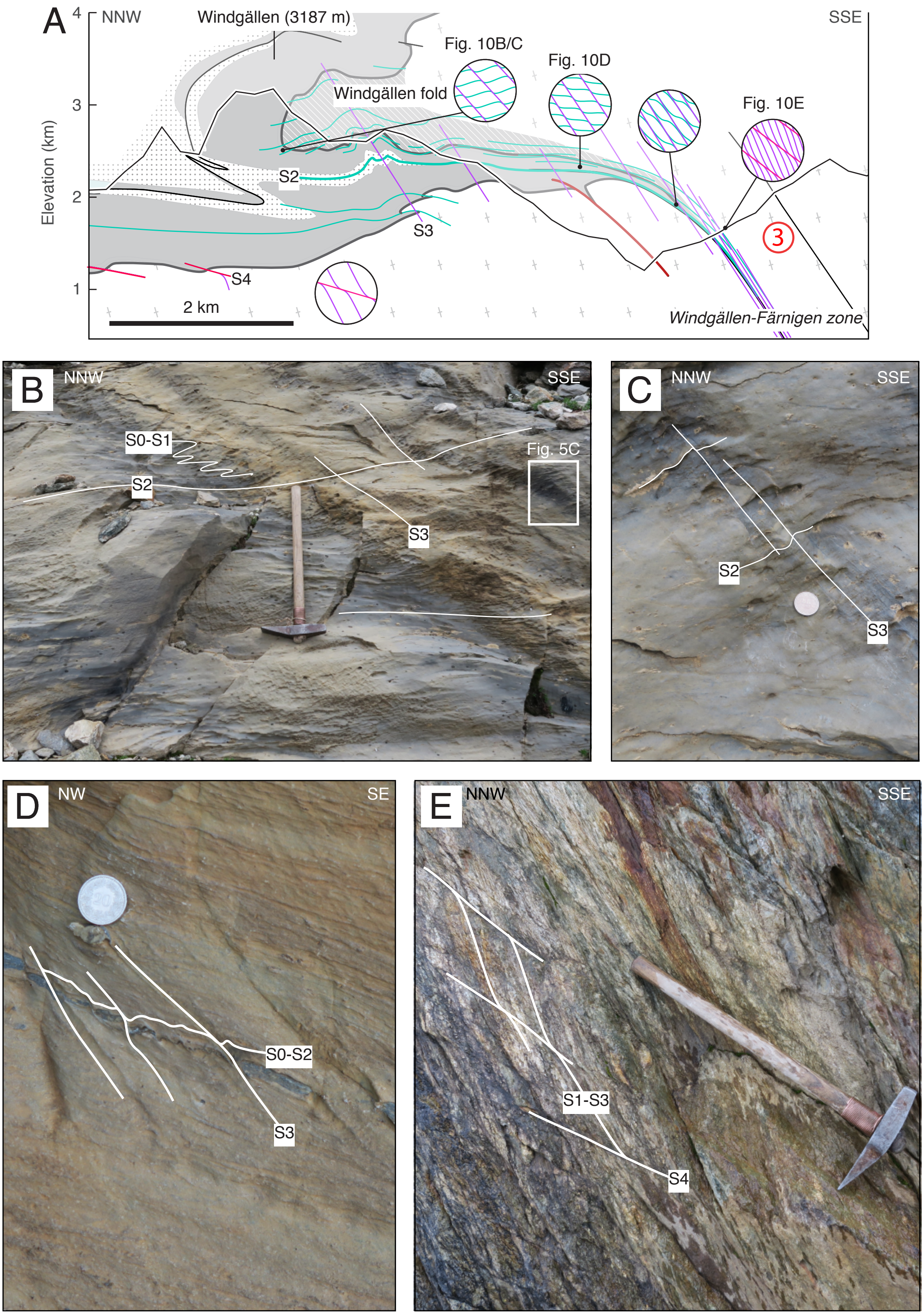

Fig. 2-12: Overprinting relationships in the Windgällen area (see Nibourel et al., 2021 for details).

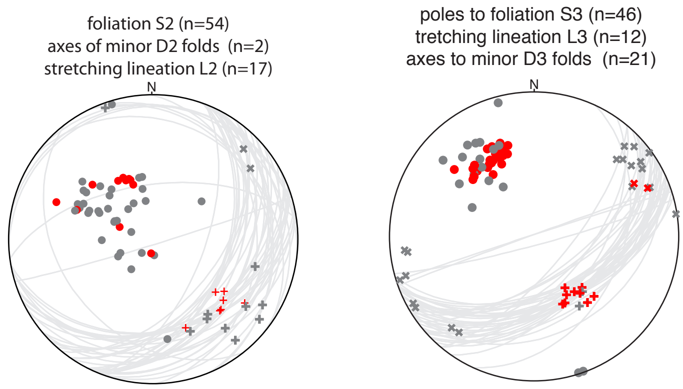

Fig. 2-13: S2 and S3 and associated stretching lineations in the Windgällen region (see Nibourel et al., 2021 for details).

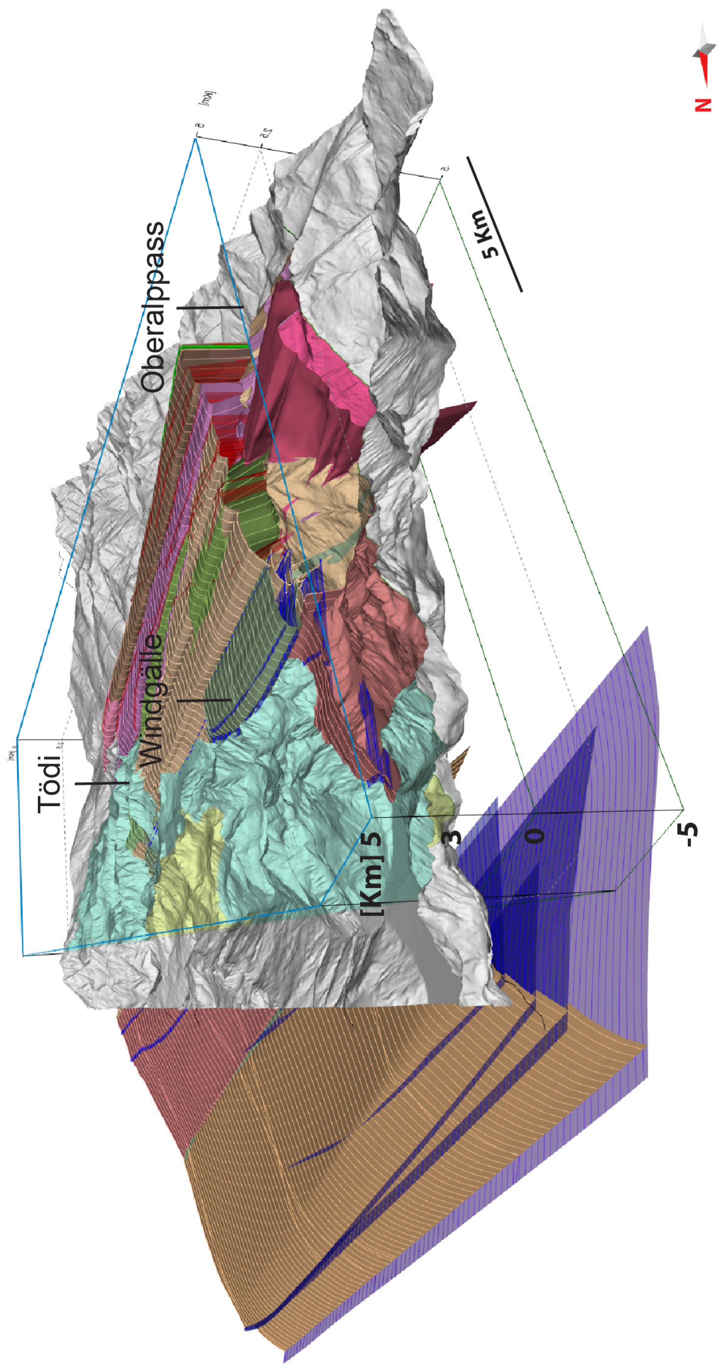

Fig. 2-14: 3D Block Diagramm of the Central to Eastern Aar Massif (by Ferdinando Musso Piantelli)

Day 2, Stop 4 Schöllenenschlucht-Andermatt

Topics:
- Alpine structures in the southernmost Aar Massif
- Contact to Mesozoic sediments of the Urseren-Garvera Zone (cover Gotthard)
- Alpine greenschist metamorphism
- Where do the Helvetic Nappes root?
- Exhumation dynamics along the Reusstal transect
- Orogen-parallel migration of peak exhumation rates

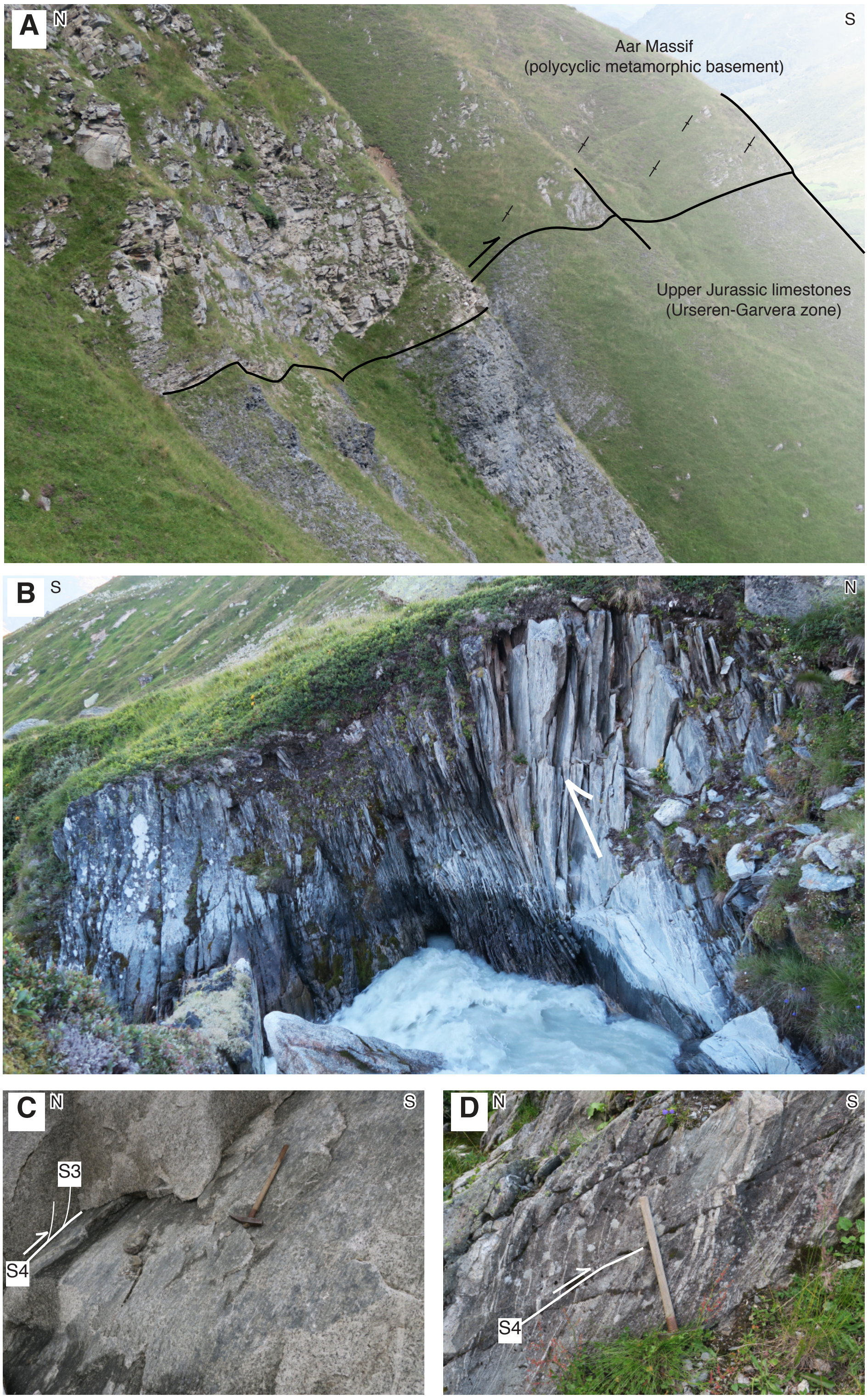

Fig. 2-15: Southernmost Aar Massif and contact to the Gotthard Nappe sediments of the Urseren-Garvera zone (see Nibourel et al., 2021 for details).

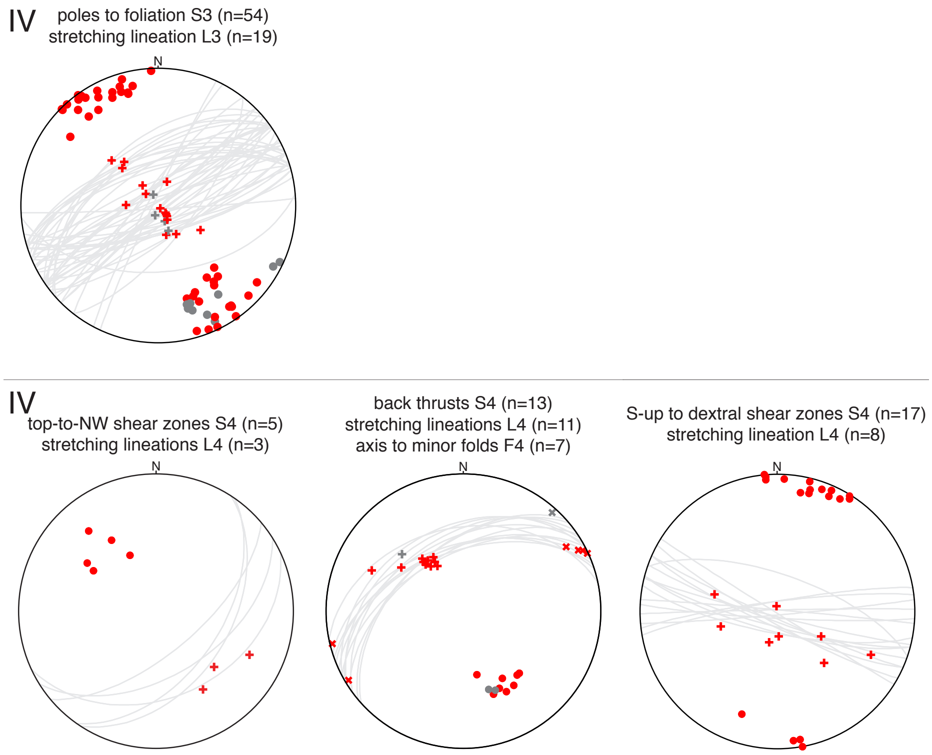

Fig. 2-16: Structural data from the central and southern Aar Massif (see Nibourel et al., 2021 for details).

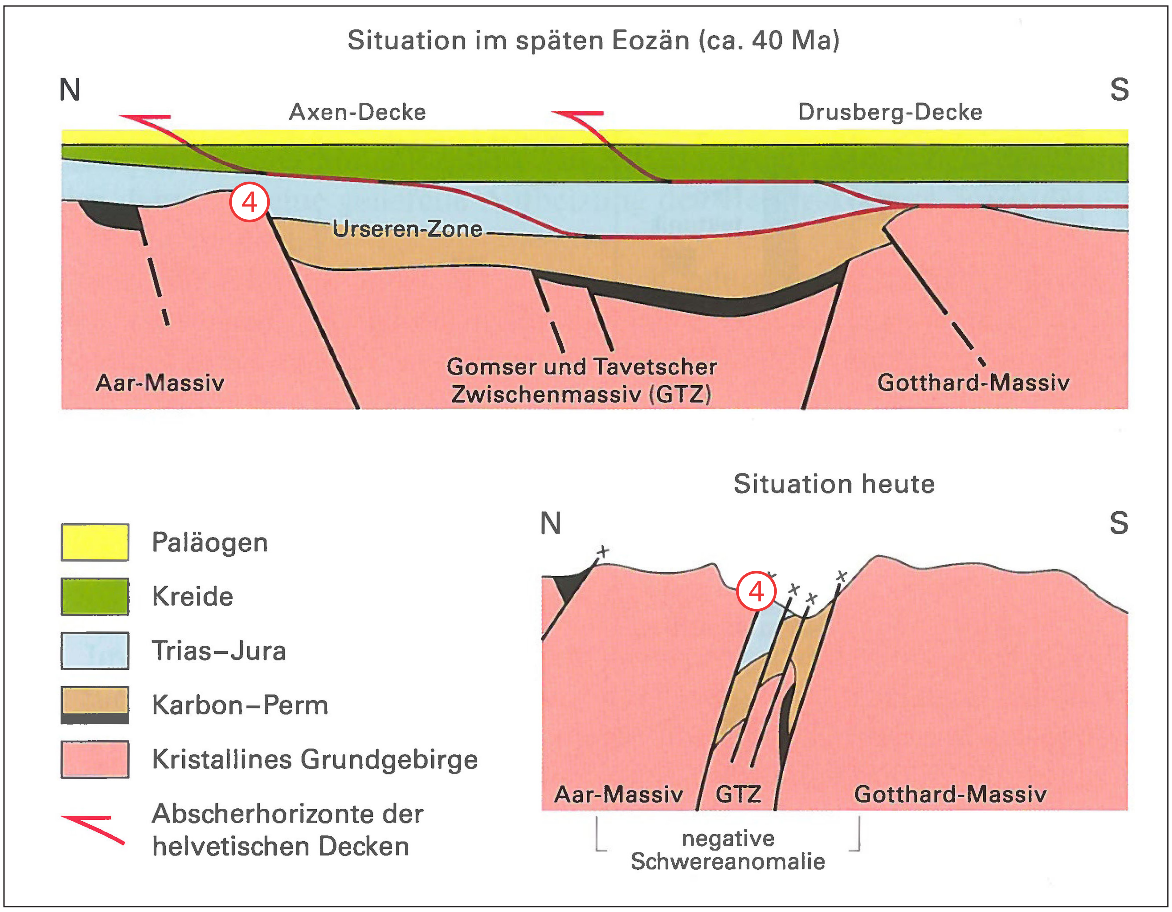

Fig. 2-17: Tectonic evolution and provenance of the allochtonous Helvetic Nappes along the Reuss Valley transect. From Labhard and Renner (2012), after Wyss (1986) and Spillmann et al. (2011). The approximate position of excursion stop 4 is indicated.

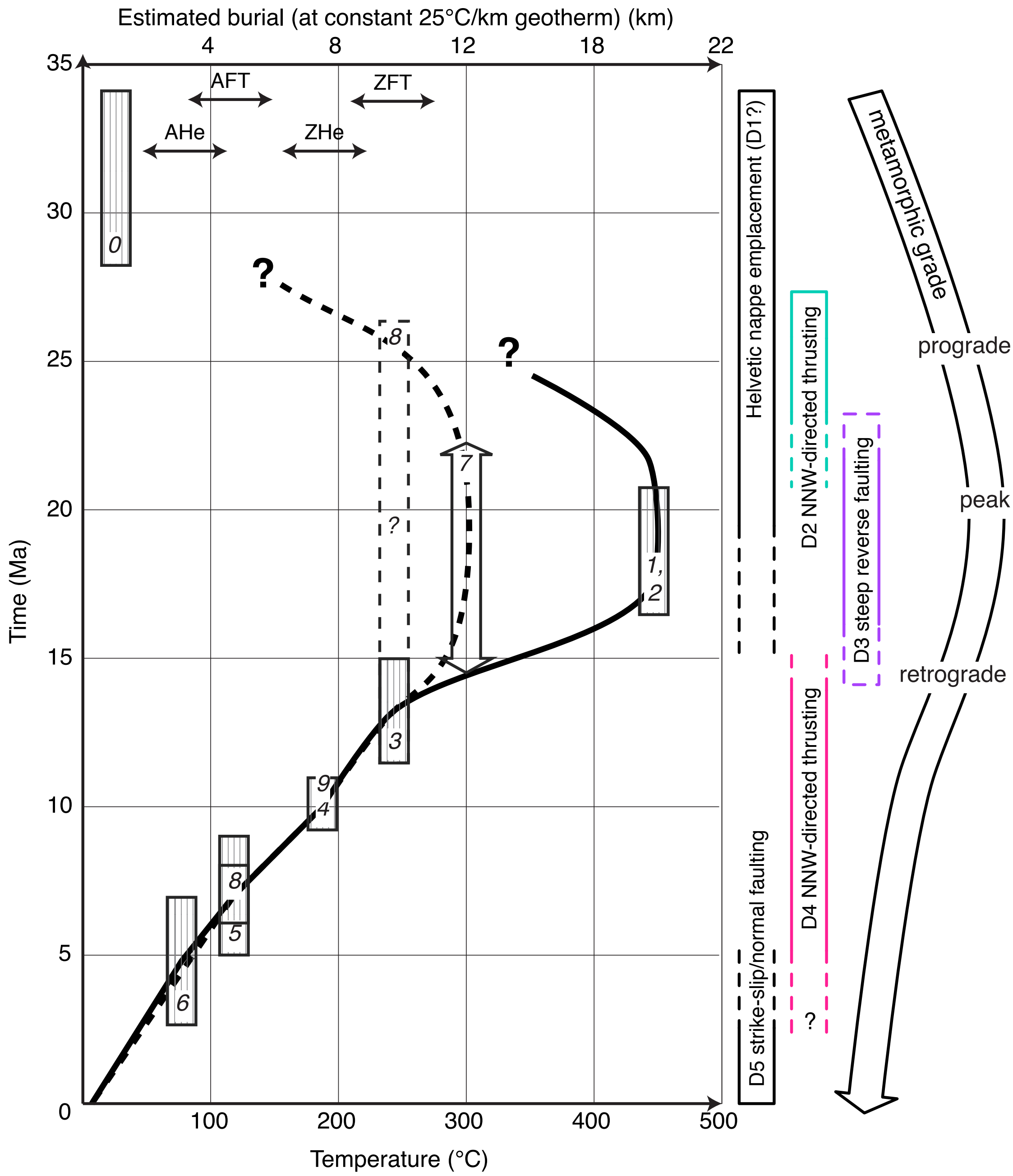

Fig. 2-18: Temperature-time-deformation history along the Reuss Valley transect (see Nibourel et al., 2021 for details).

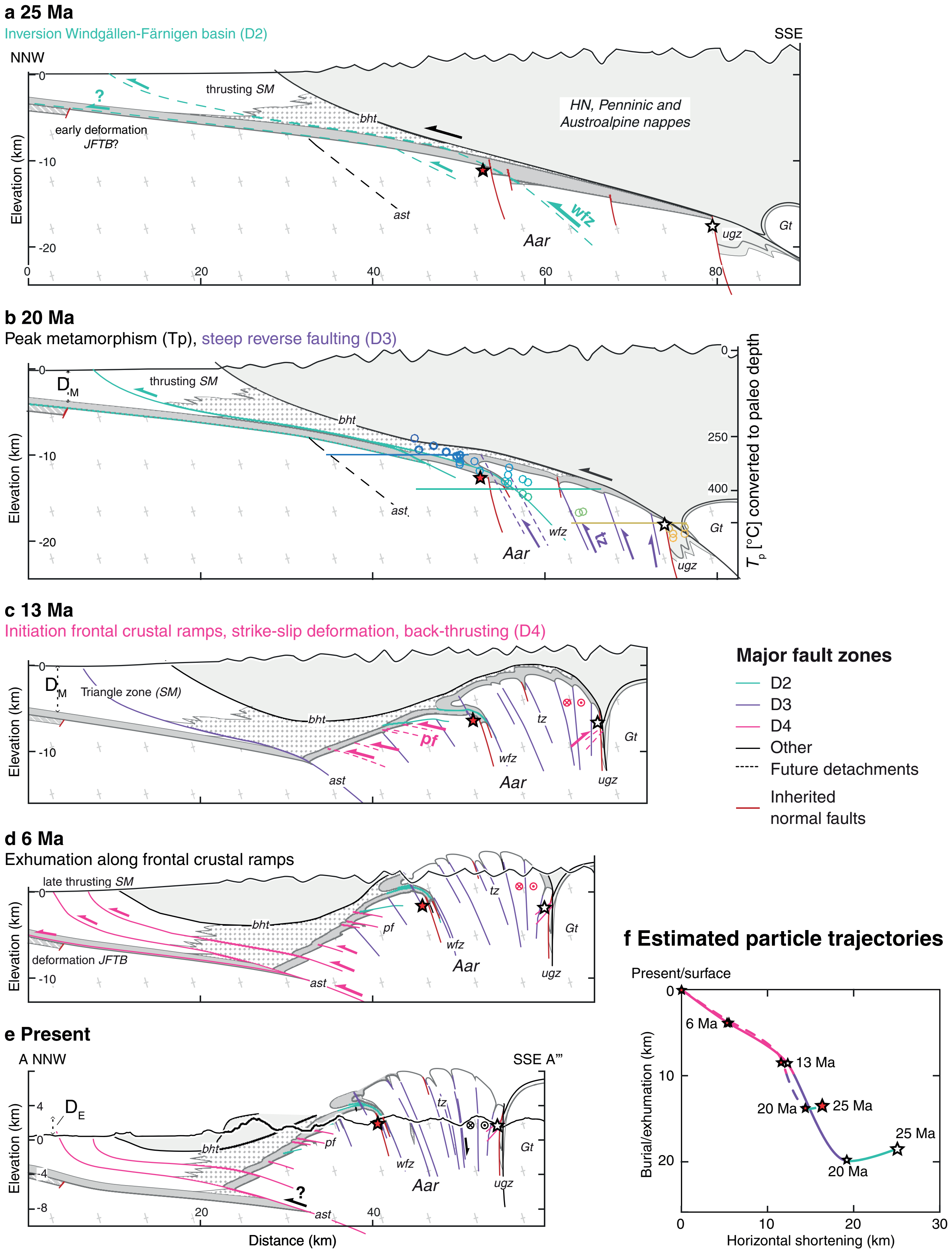

Fig. 2-19: (a-e) Suggested kinematic scenario for the Reuss Valley transect and (f) estimated particle trajectories (see Nibourel et al., 2021 for details).

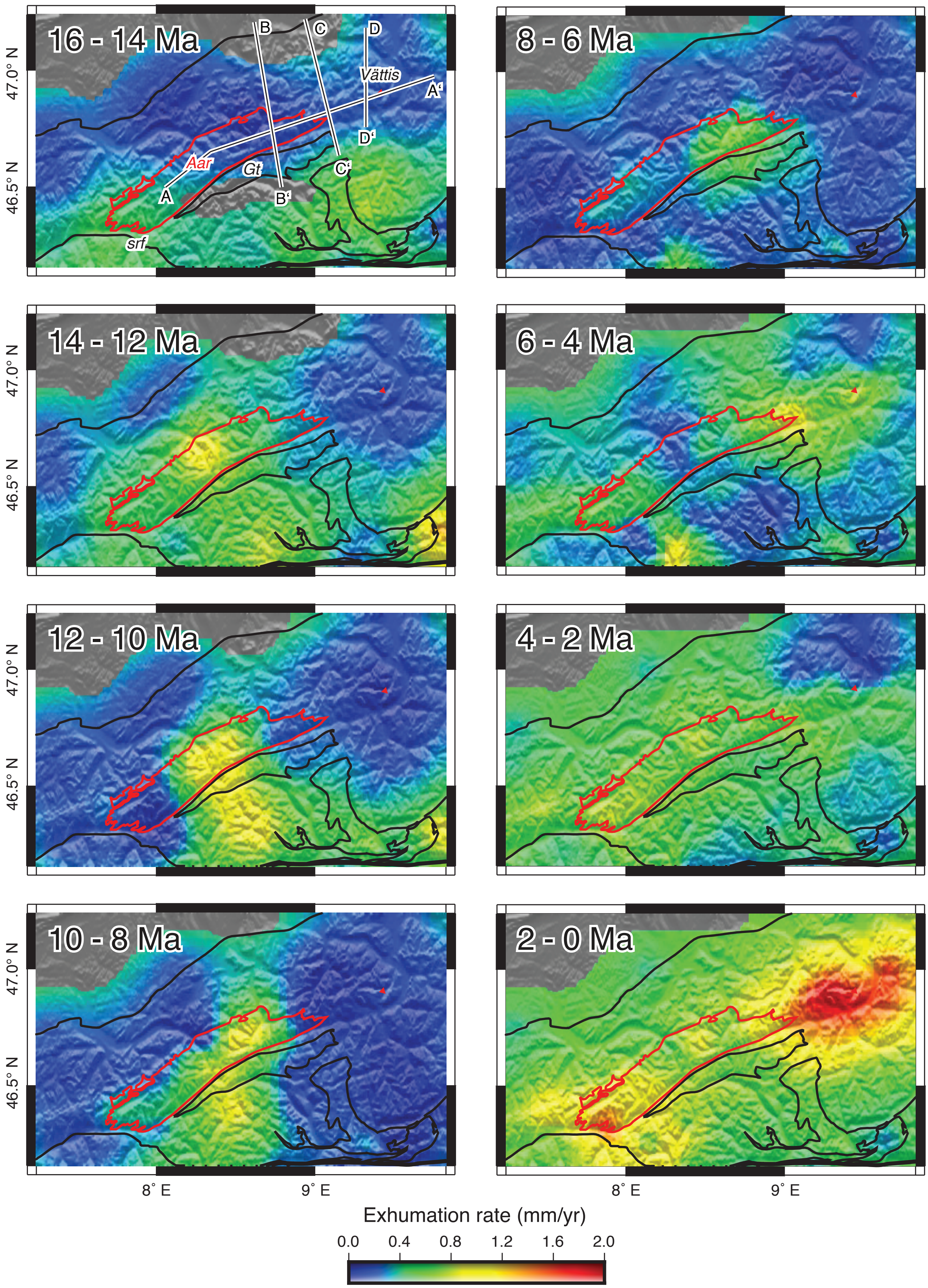

Fig. 2-20: Thermochronology-derived modeled space-time evolution of exhumation rates in the Aar Massif over the past 16 Ma (see Nibourel et al., accepted, for details).

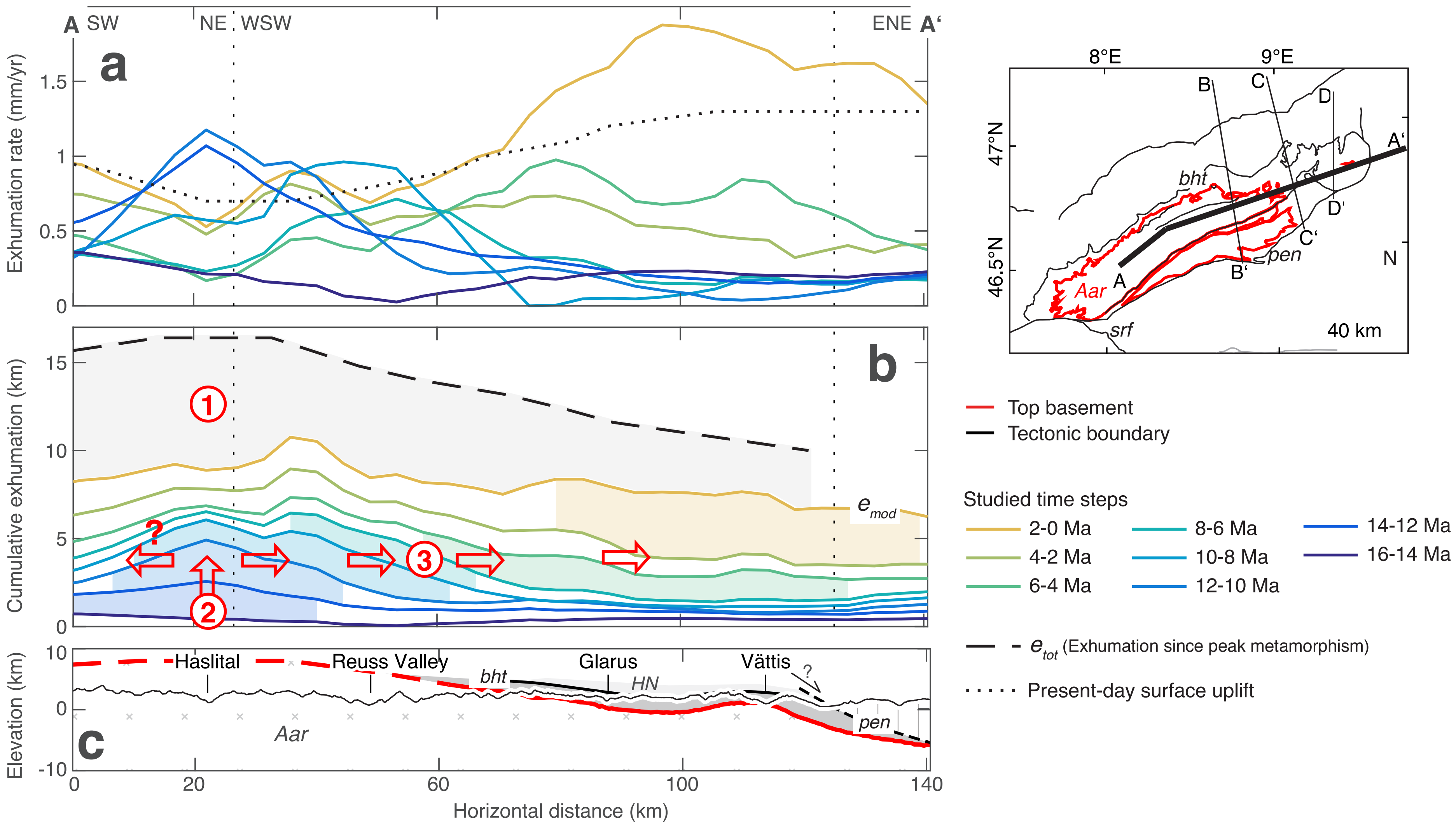

Fig. 2-21: (a) Modelled exhumation rates, present-day surface uplift rates (Schlatter, 2014) and (b) cumulative exhumation calculated for 2 Myr time steps over the past 16Ma along section A-A'. Regions of accelerated exhumation are shaded. The total exhumation since Alpine peak temperature conditions is inferred from depth-converted peak metamorphic temperature data (Figure 2). The red "1" highlights early exhumation from the moment of peak metamorphic conditions to 16Ma (grey area). Red "2" highlights the rapid exhumation restricted to the central Aar Massif from 16 to 10 Ma. Red "3" highlights eastward migration of exhumation from 10Ma to present. (c) Structural relief and major detachments along section A-A'. Legend and abbreviations as on Fig. I-1. See Nibourel et al., accepted, for details.

Day 2, Stop 5

Topics: - Isoclinal folds in the Mesozoic strata of the Windgällen-Färnigen zone
- Top basement geometry

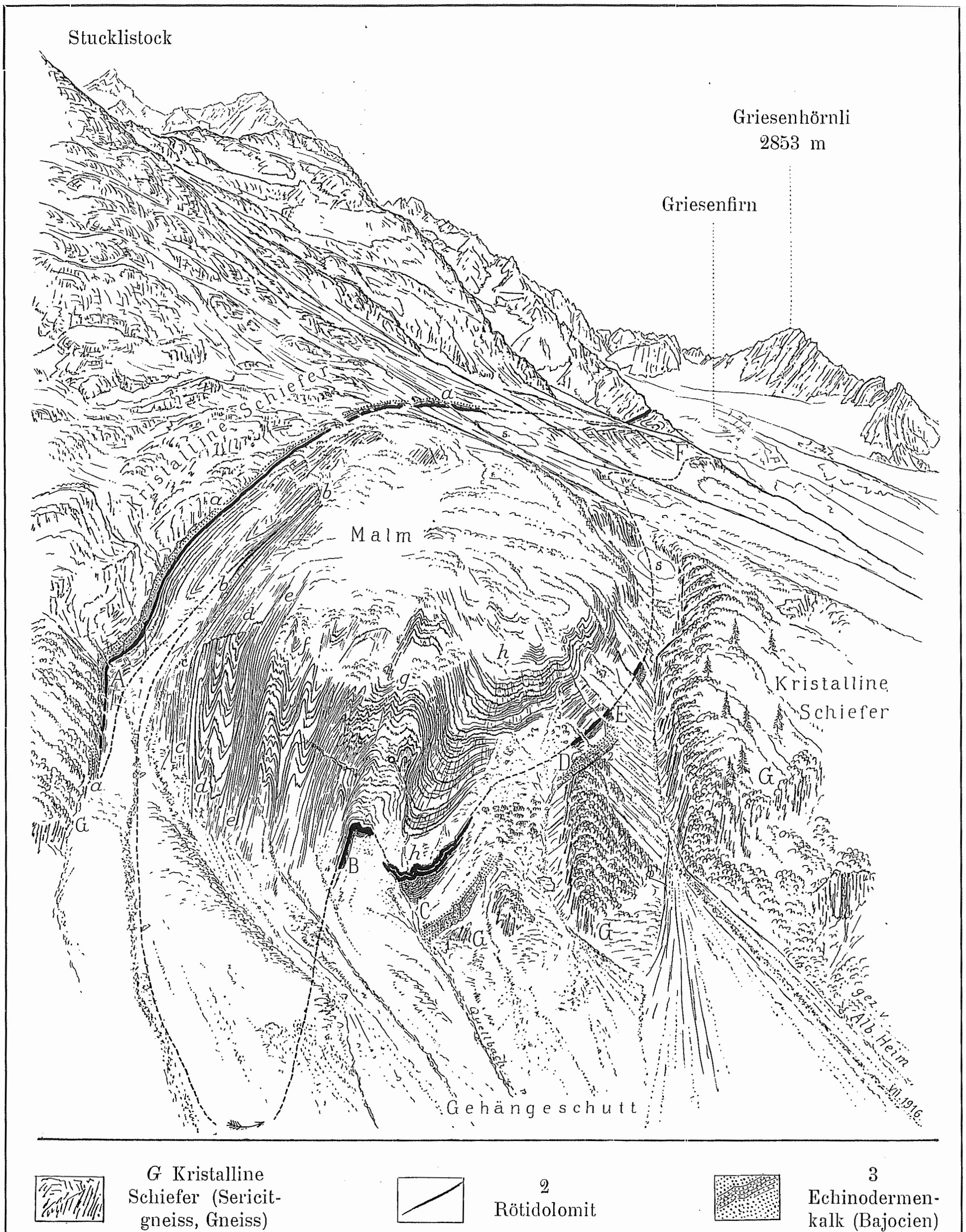

Fig. 2-22: Windgällen-Färnigen zone seen from Färnigen, Meiental (Heim and Heim,1916, coordinates: 46.73672°N, 8.51987°E).

Day 2, Stop 6

Topics:

- Weakly reactivated inherited normal faults in the Färnigen area
- Northern sediment wedge with sub-vertical foliation
- Southern sediment wedge with isoclinal folds, overturned stratigraphy and adjacent basement shear zone
- Open questions: southern sediment wedge bound by second normal fault?
- Stratigraphic age of sandstone boudins?
- Presence of Cretaceous and Permo-Carboniferous strata?

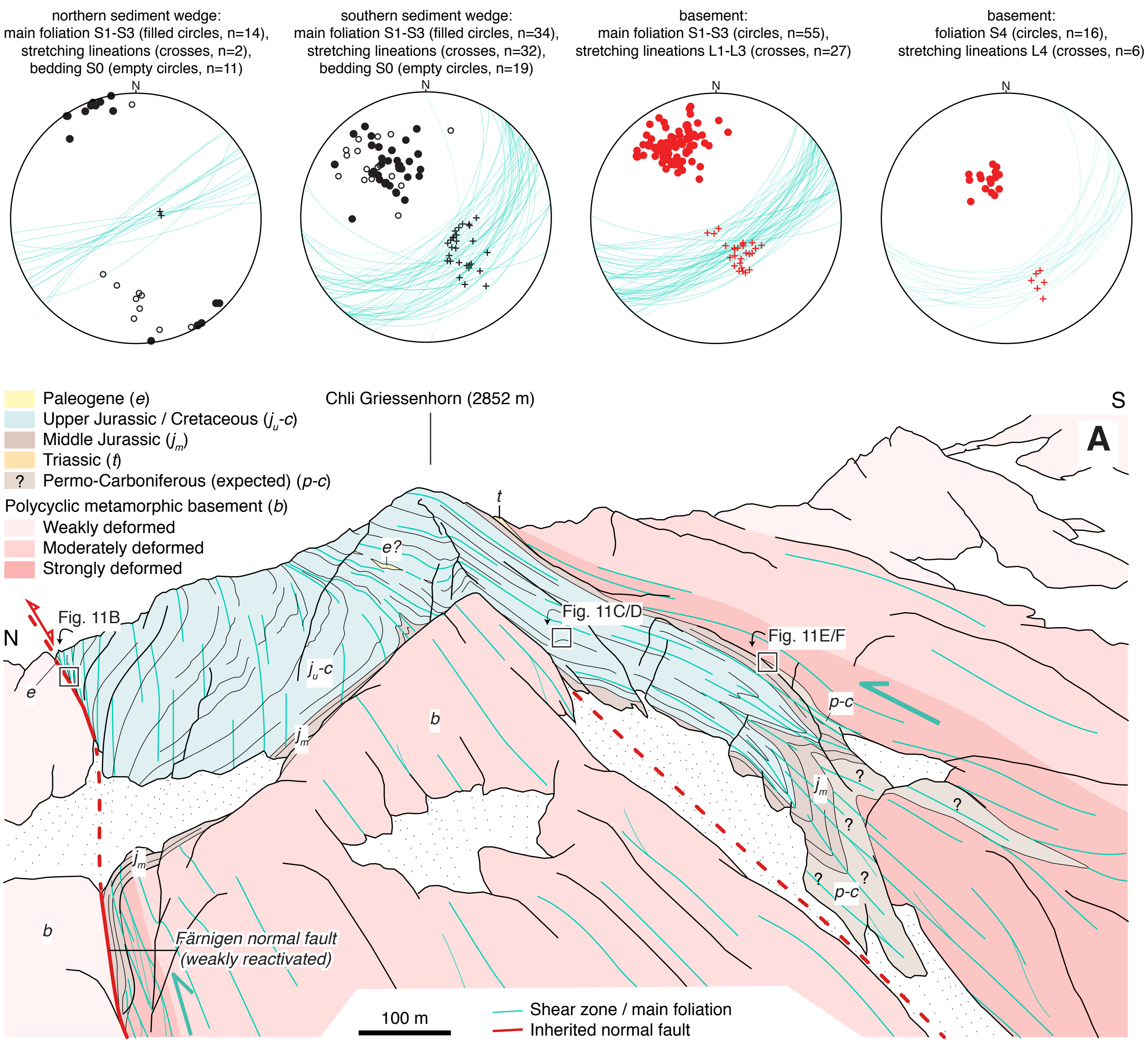

Fig. 2-23: Profile-like view of the Windgällen-Färnigen zone near Susten Pass (see Nibourel et al., 2021 for details, coordinates: 46.72661°N, 8.45418°E).

Day 3, Windgällen-Färnigen zone, Chli Griessenhorn

Topics:
- Inherited normal faults, associated half-grabens and Alpine inversion
- Overprinting relationships
- Different deformation behaviour of different lithostratigraphic units
- Late-Alpine brittle strike-slip and normal faults in limestone (D5)

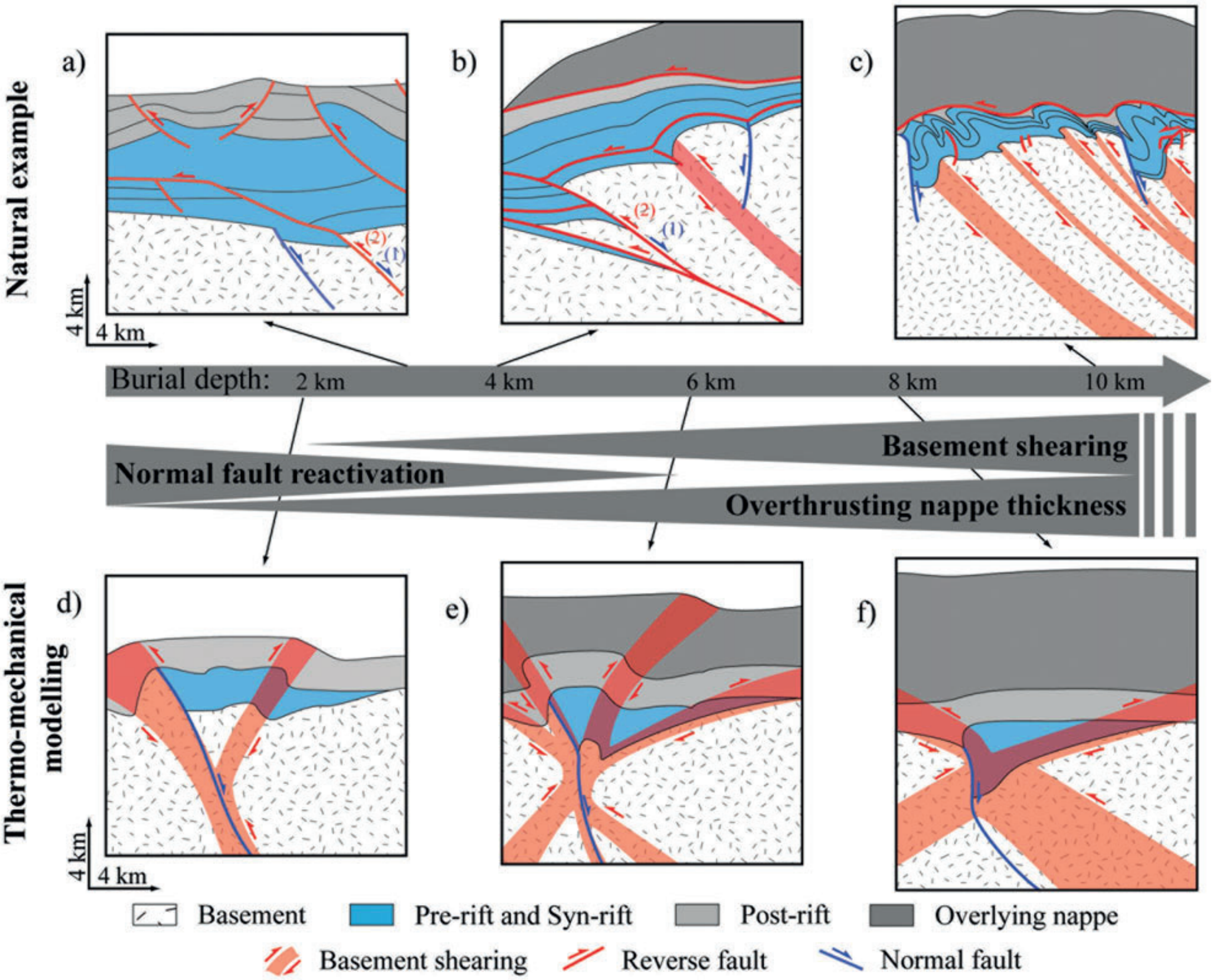

Fig. 3-1: Style of inversion in inherited half-grabens depending on the temperature conditions at deformation. (a-c) Natural examples from the Western external Alps and (d-f) numerical models. See Lafosse et al. (2016).

(Next Page) Fig. 3-2: Geological Map of the Färnigen zone between Färnigen and Susten Pass (L. Nibourel, unpublished). Excursion stops are highlighted.

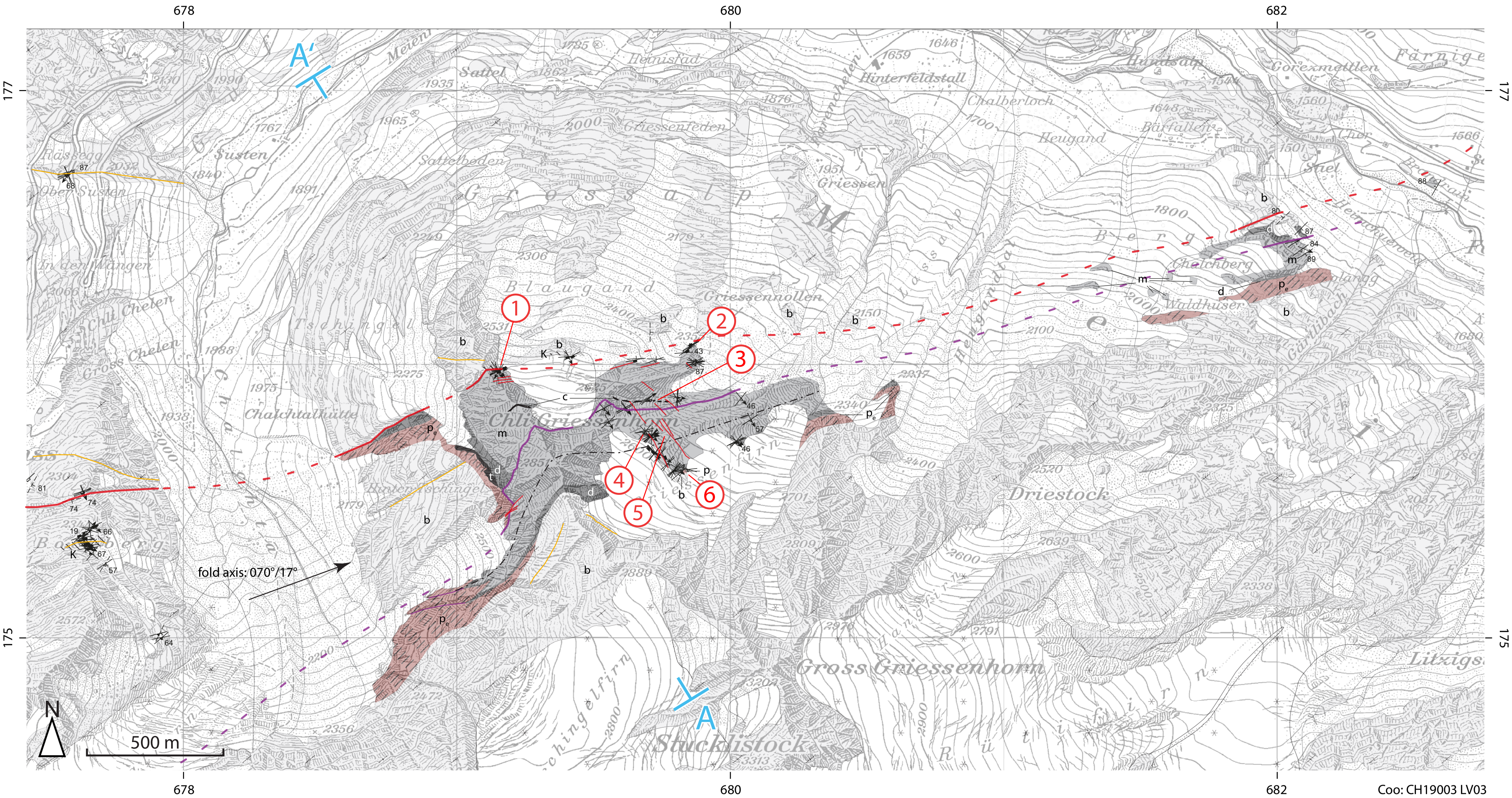

- Quaternary
- Ice
- Cenozoic (Paleocene/Eocene?)
- Upper Jurassic (Malm) (incl. Cretaceous?)
- Middle Jurassic (Dogger)
- Triassic
- Permo-Carboniferous
- Permo-Carboniferous, expected [4,5]
- Pre-Carboniferous polycyclic metam. basement
- Cataclasite, cohesive
- Alpine fault zone, > 2m, < 2m, expected
- Alpine shear zone, > 2m, < 2m, exp.
- Main Alpine foliation
- Pre-Carboniferous fault
- Fold axis
- Pre-Alpine foliation (Spre)
- Bedding (S0, dip angle)
- Main Alpine foliation (Sn, Sn+1, dip angle)
- Brittle-ductile shear zone (dip angle)
- Brittle fault (dip angle)

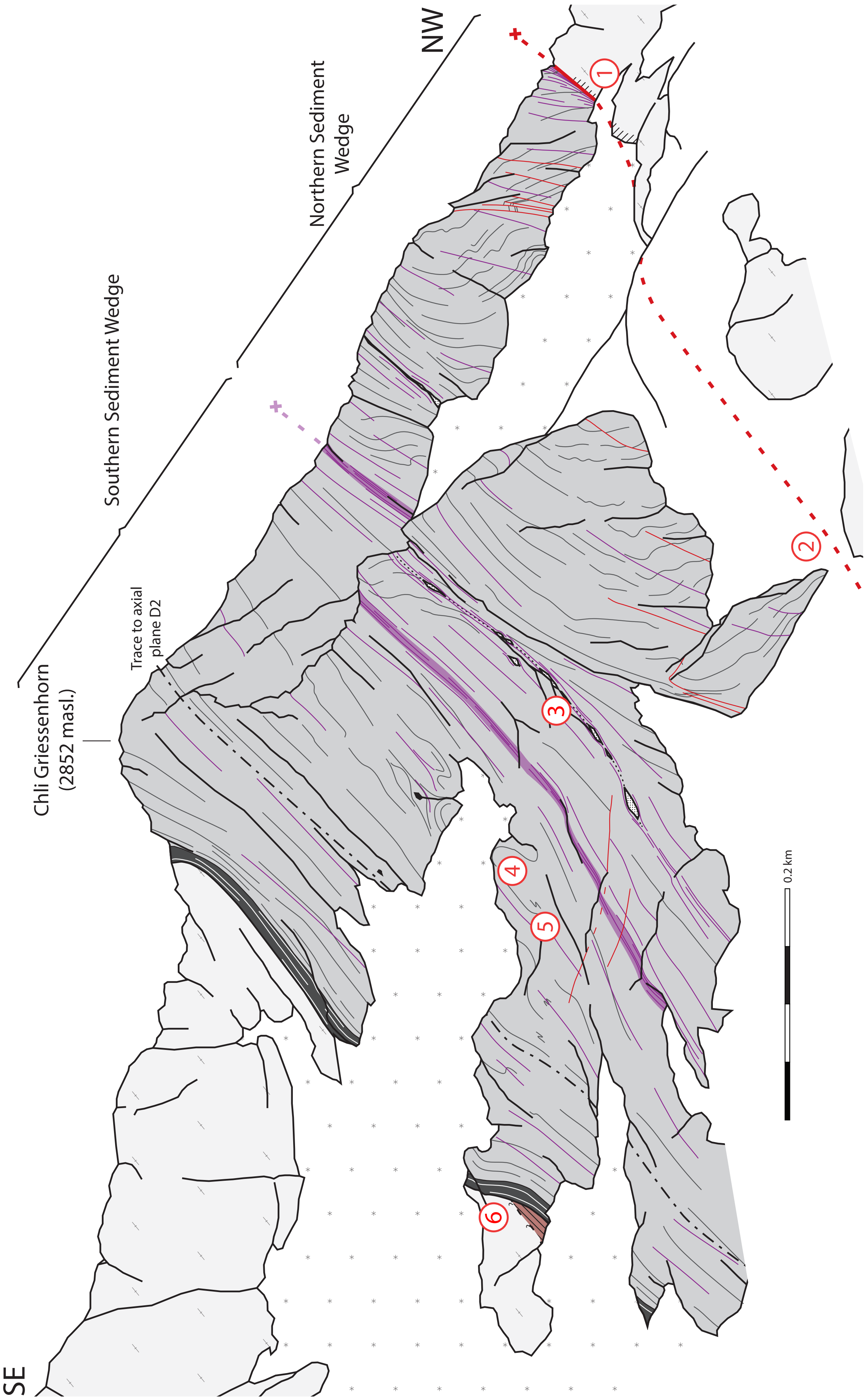

Fig. 3-3: View of the Färnigen zone west of Färnigen, seen from the NE. Excursion stops are highlighted. Legend as on Fig. 3.2

Day 3, Stop 1

Topics:
- Weakly reactivated inherited Färnigen normal fault
- Timing of normal faulting
- Stratigraphic age of thin sandstone band

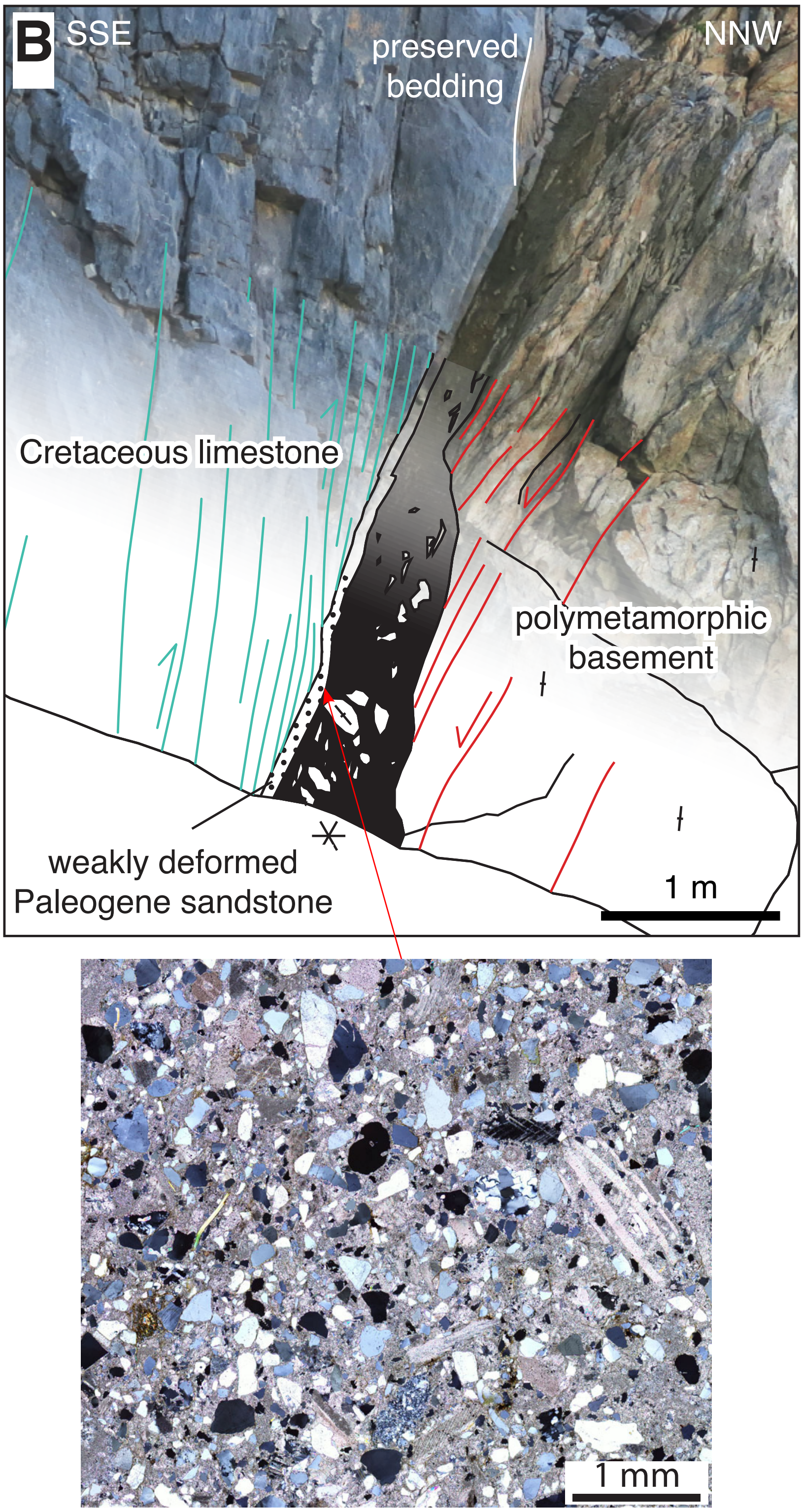

Fig. 3-4: Färnigen normal fault (coordinates: 46.73033°N, 8.47396°E). Thin section image shows the thin sandstone band at the tectonic contact to the basement. The presence of large Foraminifera (Nummulites?) indicates a Paleogene age of the sandstone.

Day 3, Stop 2

Topics: - Weakly deformed northern sediment wedge
- subvertical main foliation, pressure solution

Fig. 3-5: Chli Griessenhorn from the NE. Note the subvertical foliation in the less deformed northern sediment wedge (the red arrow highights the outcrop, coordinates: 46.73050°N, 8.48388°E).

Day 3, Stop 3

Topics: - Strongly deformed southern sediment wedge
- gradual transition to SSE-dipping main foliation
- boudinage of sandstone layers, brecciated siliceous limestone
- indications of another normal fault?
- Stratigraphy?

Fig. 3-6: Array of up to several meters large sandstone boudins in strongly foliated limestone (coordinates: 46.72905°N, 8.48010°E).

Day 3, Stop 4

Topics: - Folding and shearing

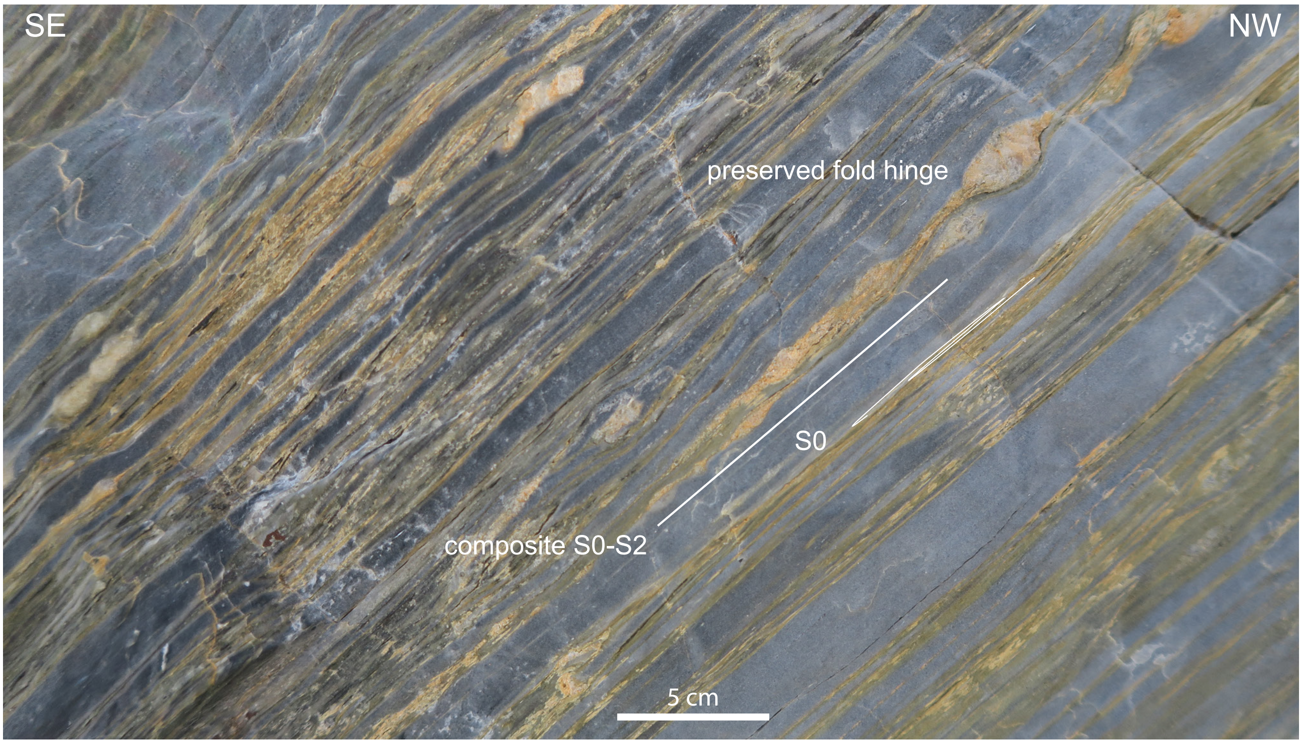

Fig. 3-7: Strongly sheared and folded mylonitic limestone. Sandy beds highlight multi-stage folding. Hinges to early folds are locally preserved (Coordinates: 46.72908°N, 8.48082°E).

Fig. 3-8: Preserved metre-scale fold hinge of siliceous limestone is internally weakly deformed. Surrounding limestone is strongly foliated (Coordinates: 46.72822°N, 8.48107°E).

Day 3, Stop 5

Topics: - Composite S0-S2 overprinted by steeper S3
- NNW-plunging stretching lineation

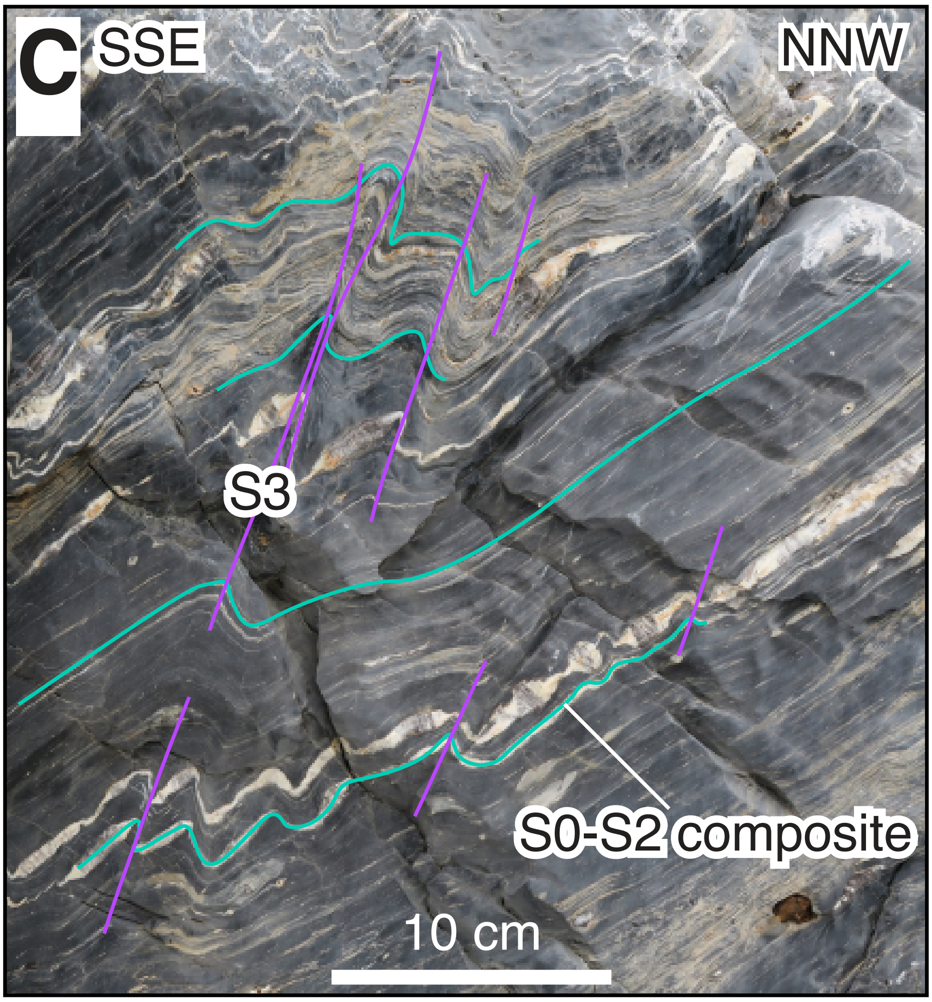

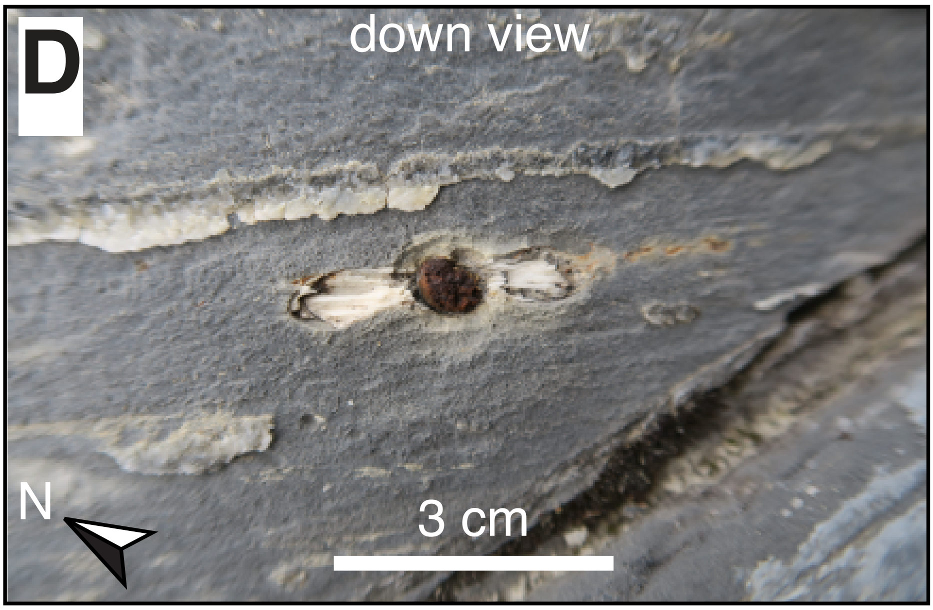

Fig. 3-9: (C) S3 overprinting an intense S0–S2 composite foliation (coordinates: 46.7281°N/8.4814°E). (D) Well-developed stretching lineation in fine-grained limestone and pressure shadow around a pyrite concretion in the main foliation surface (S0–S3 composite). Coordinates: 46.7291°N/8.4850°E). See Nibourel et al. (2021) for details.

Day 3, Stop 6

Topics: - Overturned stratigraphic contact between basal Mesozoic strata and polycyclic metamorphic basement / Permo-Carboniferous rocks
- Absence of triassic strata, dolomitic clasts in basal conglomerate

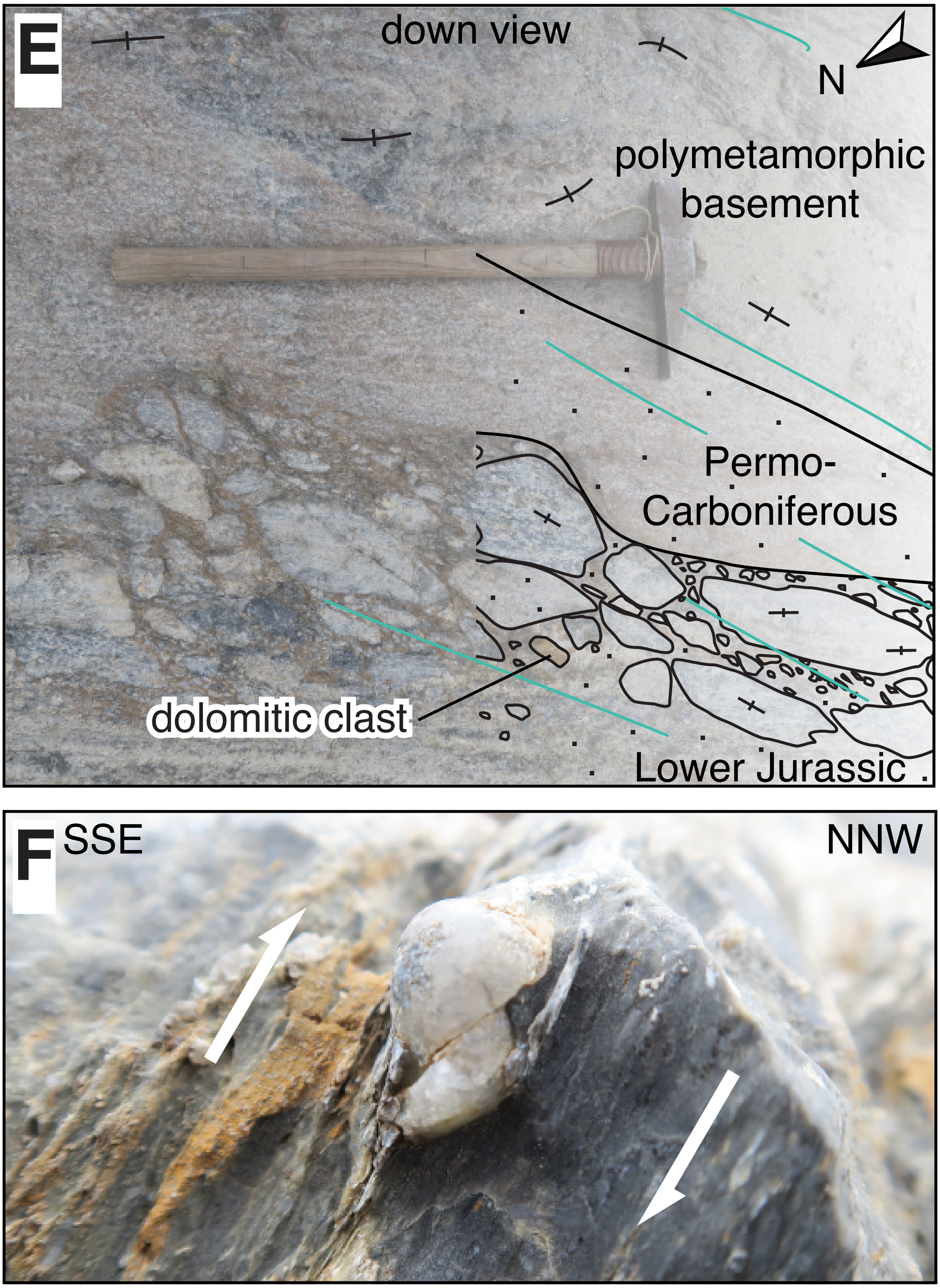

Fig. 3-10: (E) Overturned stratigraphic contacts between Carboniferous, Mesozoic sediments and the basement. The presence of dolomite clasts indicates a (Middle?) Jurassic or younger age for the basal conglomerate (Coordinates: 46.7269°N/8.4830°E). (F) Centimetre-sized shear band type fragmented quartz porphyroclast indicating top-to-the NNW shearing during D2 (coordinates: 46.7269°N/8.4830°E). See Nibourel et al. (2021) for details.

Key references:

Berger, A., Mercolli, I. P., Herwegh, M., & Gnos, E. (2017). Geological map of the Aar massif and Tavetsch and Gotthard nappe, Geol Spec. Map 129 Explanatory Notes 129.

Berger, A., Wehrens, P., Lanari, P., Zwingmann, H., & Herwegh, M. (2017). Microstructures, mineral chemistry and geochronology of white micas along a retrograde evolution: An example from the Aar massif (Central Alps, Switzerland). Tectonophysics, 721, 179-195.

Brückner, W. & Niggli, E. 1954: Bericht über die Exkursion zum Scheidnössli bei Erstfeld, in der Urserenmulde vom Rhonegletscher bis Andermatt und ins westliche Tavetscher Zwischenmassiv. Eclogae geol. Helv., v. 47/2: 383-401.

Brückner, W. et al. 1967: Exkursion Nr. 22: Altdorf - Gotthard - Bellinzona. p. 380-399. In: Nabholz, W. [Ed.] Geologischer Führer der Schweiz, Heft 5, Grimsel-Susten-Simplon-Gotthard-Lukmanier und Tessin, Exkursionen Nr. 19-26; 406 pp., Wepf & Co.

Funk, H.P. et al. 1983: Bericht über die Jubiläumsexkursion "Mechanismus der Gebirgsbildung" der Schweizerischen geologischen Gesellschaft in das ost- und zentralschweizerische Helvetikum und in das nördliche Aarmassiv vom 12. bis 17. September 1982. Eclogae geol. Helv., v. 76/1: 91-123.

Heim, A., & Heim, A. (1916). Die Juramulde in Aarmassive bei Fernigen (Uri). Geologische Nachlese, 25, 504-530.

Heim, A. & Heim, A. 1917: Der Kontakt von Gneiss und Mesozoikum am Nordrand des Aarmassivs bei Erstfeld. Geologische Nachlese Nr. 26, Vierteljahrsschrift der Naturforschenden Gesellschaft in Zürich, v. 62, p. 423-451.

Herwegh, M., Berger, A., Baumberger, R., Wehrens, P., & Kissling, E. (2017). Large-scale crustal-block-extrusion during late Alpine collision. Scientific reports, 7(1), 1-10.

Herwegh, M., Berger, A., Glotzbach, C., Wangenheim, C., Mock, S., Wehrens, P., ... & Kissling, E. (2020). Late stages of continent-continent collision: Timing, kinematic evolution, and exhumation of the Northern rim (Aar Massif) of the Alps. Earth-science reviews, 200, 102959.

Janots, E. et al. 2009: Metamorphic rates in collisional orogeny from in situ allanite and monazite dating. Geology, v. 37, p. 11-14.

Janots, E. et al. 2012: Constraints on fluid evolution during metamorphism from U–Th–Pb systematics in Alpine hydrothermal monazite. Chemical Geology, v. 326-327, p. 61-71.

Labhart, T. & Renner, F. 2012: Blatt 1231 Urseren. – Geol. Atlas Schweiz 1:25 000, Erläut. 133, swisstopo, 152 p.

Labhart, T., Gisler, C., Renner, F., Schwizer, B., & Schaltegger, U. 2015: Blatt 1211 Meiental. – Geol. Atlas Schweiz 1:25 000, Erläut. 146, swisstopo.

Lafosse, M., Boutoux, A., Bellahsen, N., & Le Pourhiet, L. (2016). Role of tectonic burial and temperature on the inversion of inherited extensional basins during collision. Geological Magazine, 153(5-6), 811-826.

Mock, S., von Hagke, C., Schlunegger, F., Dunkl, I., & Herwegh, M. (2020). Long-wavelength late-Miocene thrusting in the north Alpine foreland: implications for late orogenic processes. Solid Earth, 11(5), 1823-1847.

Nibourel, L., Berger, A., Egli, D., Luensdorf, N. K., & Herwegh, M. (2018). Large vertical displacements of a crystalline massif recorded by Raman thermometry. Geology, 46(10), 879-882.

Nibourel, L. (2019). The structural and thermo-kinematic evolution of the eastern Aar Massif, Switzerland. Ph.D. thesis, unpublished, Universität Bern

Nibourel, L., Berger, A., Egli, D., Heuberger, S., & Herwegh, M. (2021). Structural and thermal evolution of the eastern Aar Massif: insights from structural field work and Raman thermometry. Swiss journal of geosciences, 114(1), 1-43.

Nibourel, L., Rahn, M., Dunkl, I., Berger A., Herman F., Diehl T., Heuberger, S., & Herwegh, M. (accepted). Orogen-parallel migration of exhumation in the eastern Aar Massif revealed by low-T thermochronology. Journal of Geophysical Research, Solid Earth.

Pfiffner, O. A. (2011). Explanatory Notes to Structural map of the Helvetic zone of the Swiss Alps, including Vorarlberg (Austria) and Haute Savoie (France), Explanatory notes.

Schlunegger, F., Matter, A., Burbank, D. W., & Klaper, E. M. (1997). Magnetostratigraphic constraints on relationships between evolution of the central Swiss Molasse basin and Alpine orogenic events. Geological Society of America Bulletin, 109(2), 225-241.

Schmid, S. M., Fügenschuh, B., Kissling, E., & Schuster, R. (2004). Tectonic map and overall architecture of the Alpine orogen. Eclogae Geologicae Helvetiae, 97(1), 93-117.

Spillmann, P. et al. 2011: Geologie des Kantons Uri. Naturforschende Gesellschaft Uri - Bericht Nr. 24, 224p.

Trümpy R., 1980: An outline of the geology of Switzerland. Wepf & Co.

Trümpy, R. & Trommsdorff, V. 1980: Alps of Eastern Switzerland. Excursion No. IV. In: Trümpy, R. et al. (Eds.) - Geology of Switzerland, a guide book, Part B: Geological excursions. p. 211-260.

Wyss, R. 1986: Die Urseren-Zone – Lithostratigraphie und Tektonik. Eclogae geol. Helv., v. 79/3, p. 731-767.

Anhang A1

Attempt to correlate deformation phases with previous work:

Domain	References	Deformation phases				
Eastern Aar Massif	This study	D1	D2	D3	D4	D5
	Funk et al. (1983), Schenker (1980), Brückner and Zbinden (1987)	Griessstock and Kammlistock nappe emplacement, Helvetic Nappe emplacement, Hochfulen phase	Windgällen phase	Schwarzstöckli phase	–	–
	Milnes and Pfiffner (1977)	Cavestrau phase?	Calanda phase?	Calanda phase? Ruchi phase	–	–
Central Aar Massif	Wehrens et al. (2017), Herwegh et al. (2020)	–	–	Handegg phase	Oberaar phase, Pfaffenchopf phase	Gadmen faults
	Rolland et al. (2009)	–	–	Stage 1	stage 2, stage 3?	Stage 3?
	Burkhard (1988), Pfiffner (2015)	Kiental phase?	Kiental phase	Grindelwad phase	Grindelwad phase	–
Urseren-Garvera zone	Wyss (1986)	D1	D2	D3	Post-D3	–

Fig. A-1: Attempt to correlate deformation phases from this study with previous work. See Nibourel et al. (2021) for details.

Anhang A2-1, Structural data (Nibourel et al., 2021)

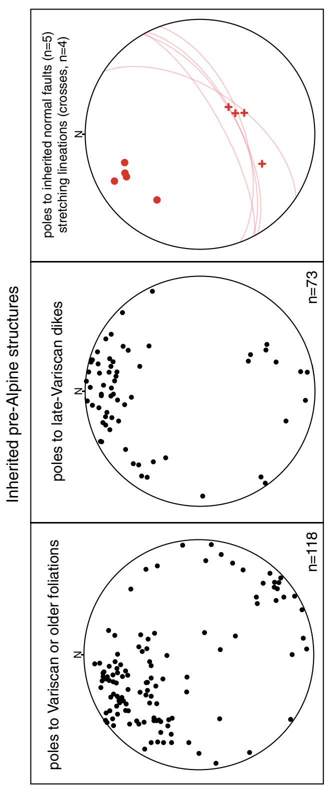

Fig. 4 Structural data related to inherited pre-collisional structures (Schmidt, lower hemisphere). n: number of measurements

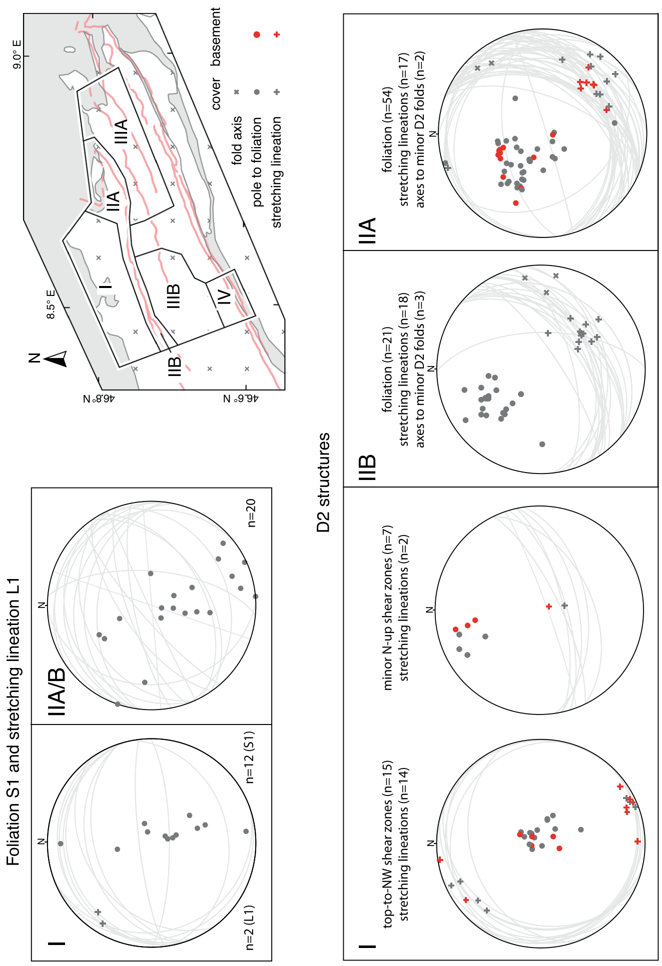

Fig. 5 Structural data related to D1 and D2. Stereographic projections of poles to foliations, lineations and fold axes are given for each subregion. n: number of measurements. Where appropriate, the projections are coded for lithologies (see legend)

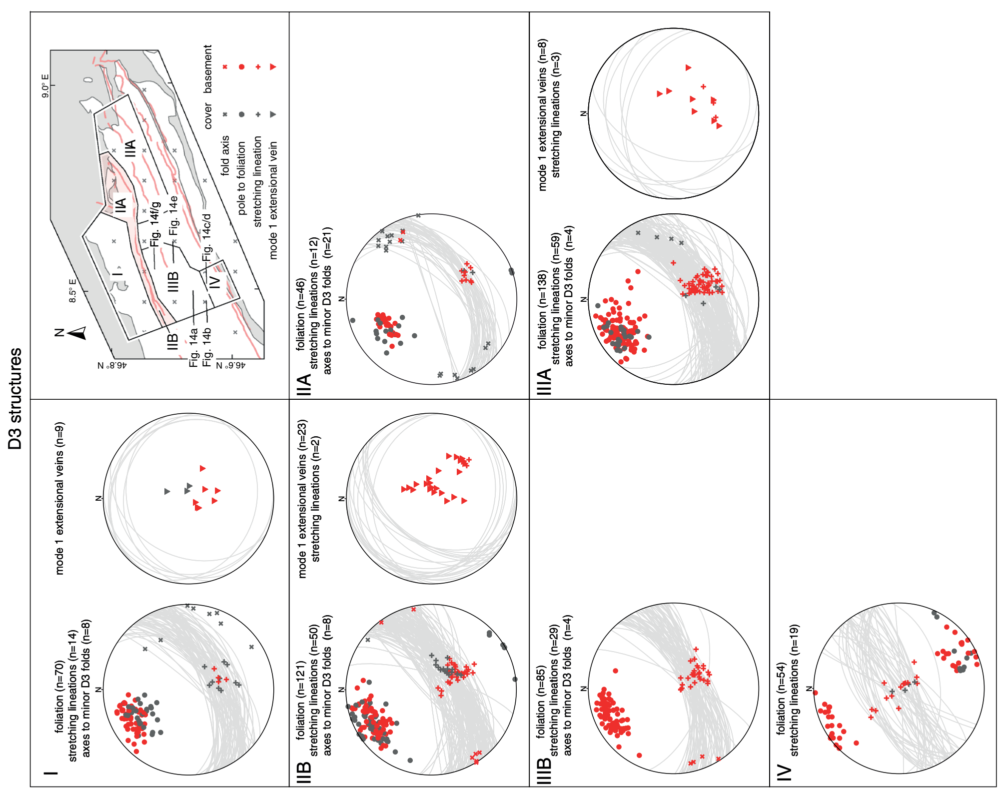

Fig. 6 Structural data related to D3. For each subregion stereographic projections of poles to planes, lineations and fold axes are given. n: number of measurements. Where appropriate, the projections are coded for lithologies (see legend)

Anhang A2-2, Structural data (Nibourel et al., 2021)

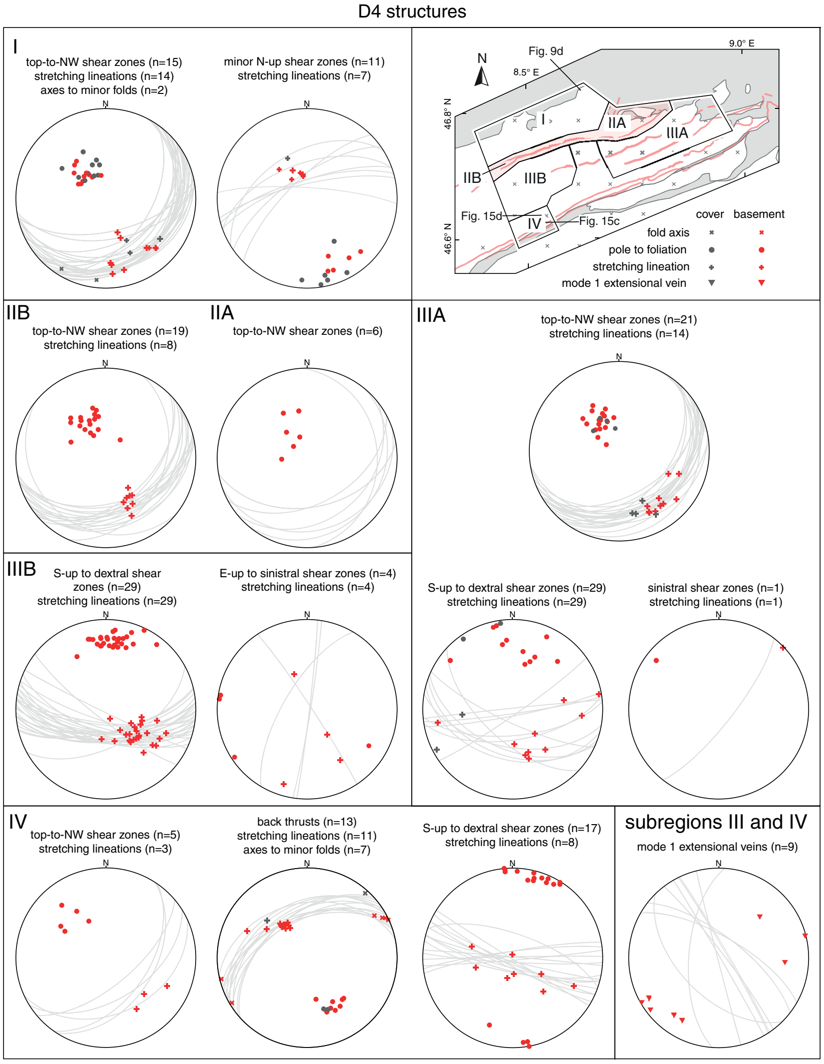

Fig. 7 Structural data related to D4. For each subregion stereographic projections of poles to planes, lineations and fold axes are given. n: number of measurements. Where appropriate, the projections are coded for lithologies (see legend)

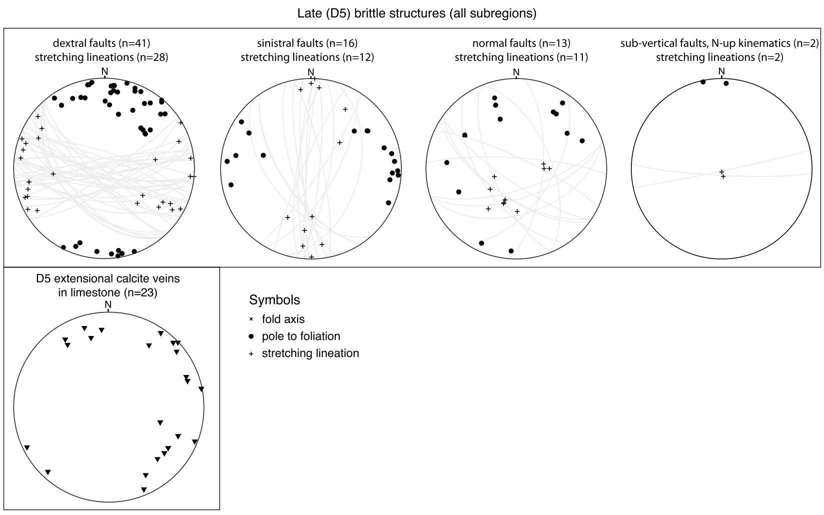

Fig. 8 Stereographic projection of late brittle faults and post-foliation late mode 1 extensional calcite veins (cover units only). n: number of measurements

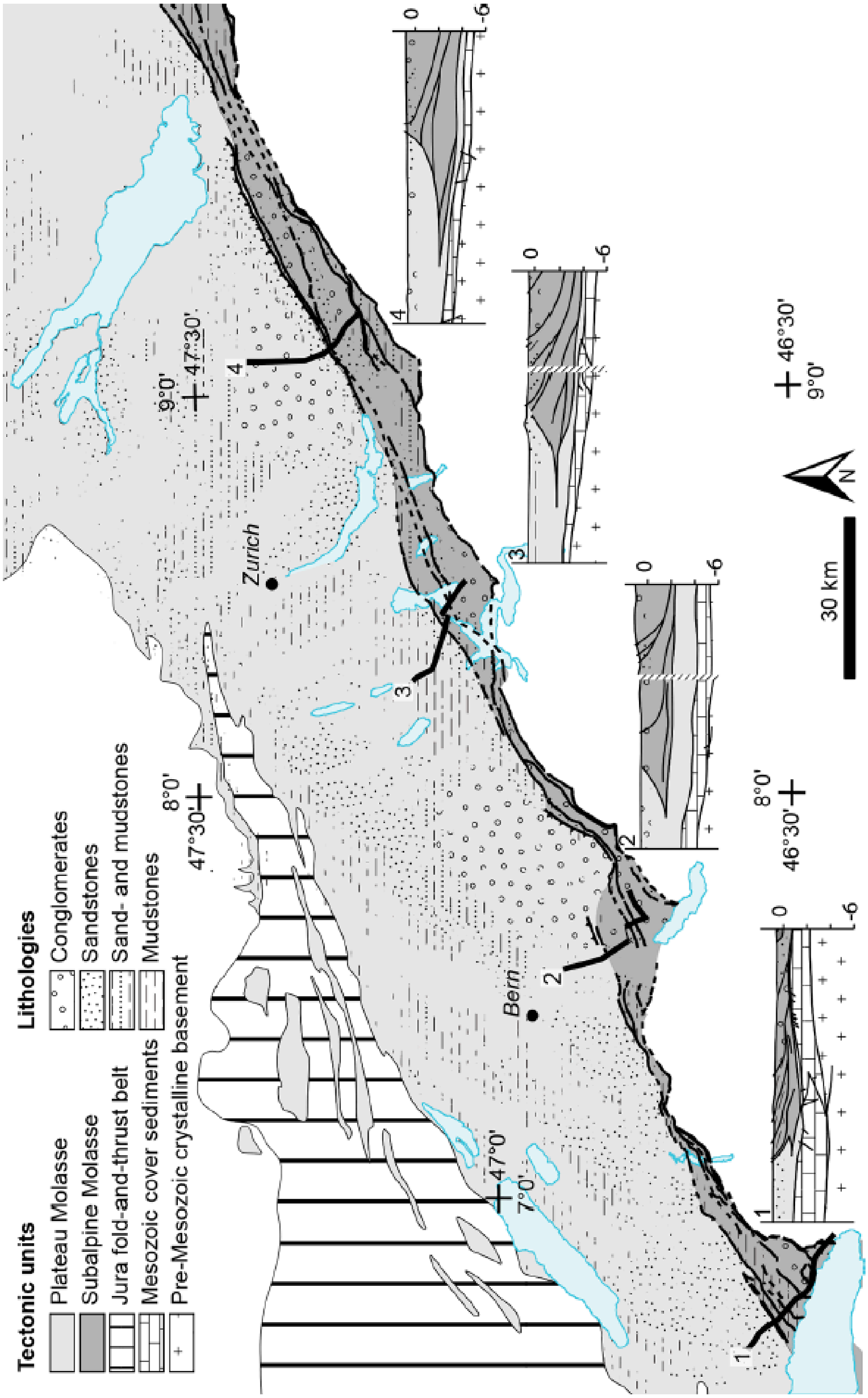

Fig. 2-6: Litho-tectonic map of the Molasse basin (for details see Mock et al. 2020).

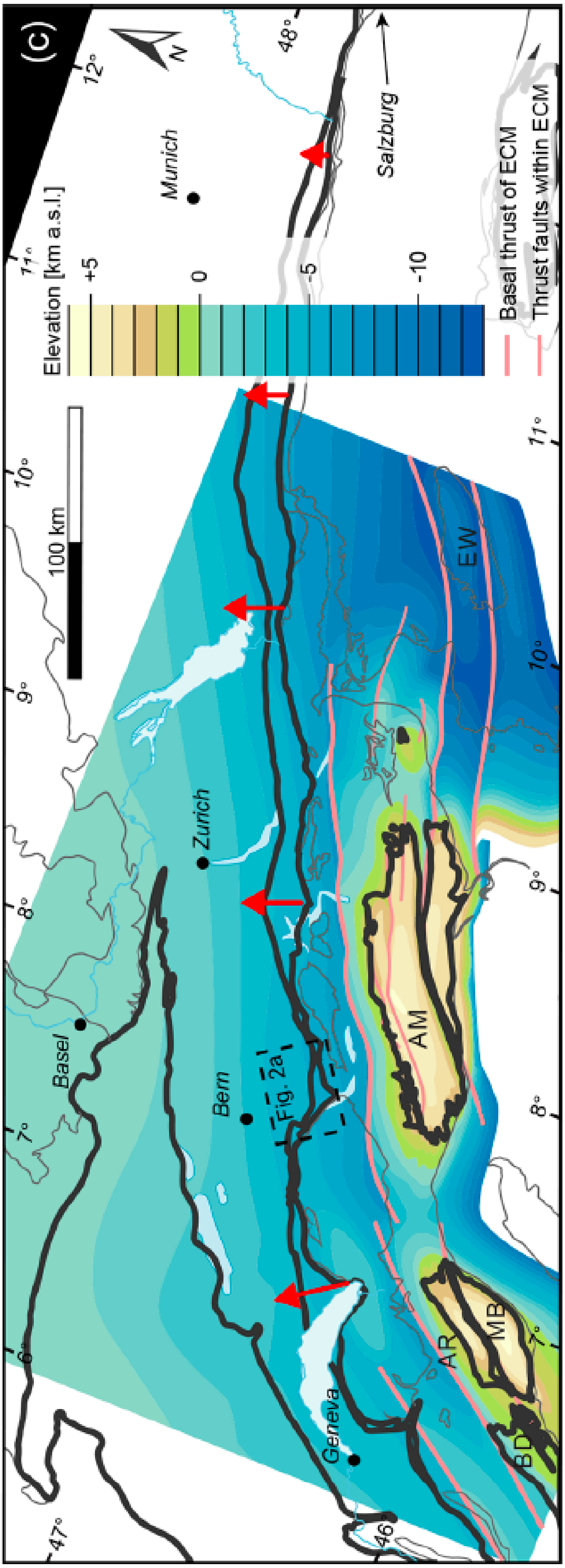

Fig. 2-8: Contour lines top basement and outline of Northalpine thrust front (for details see Mock et al. 2020).

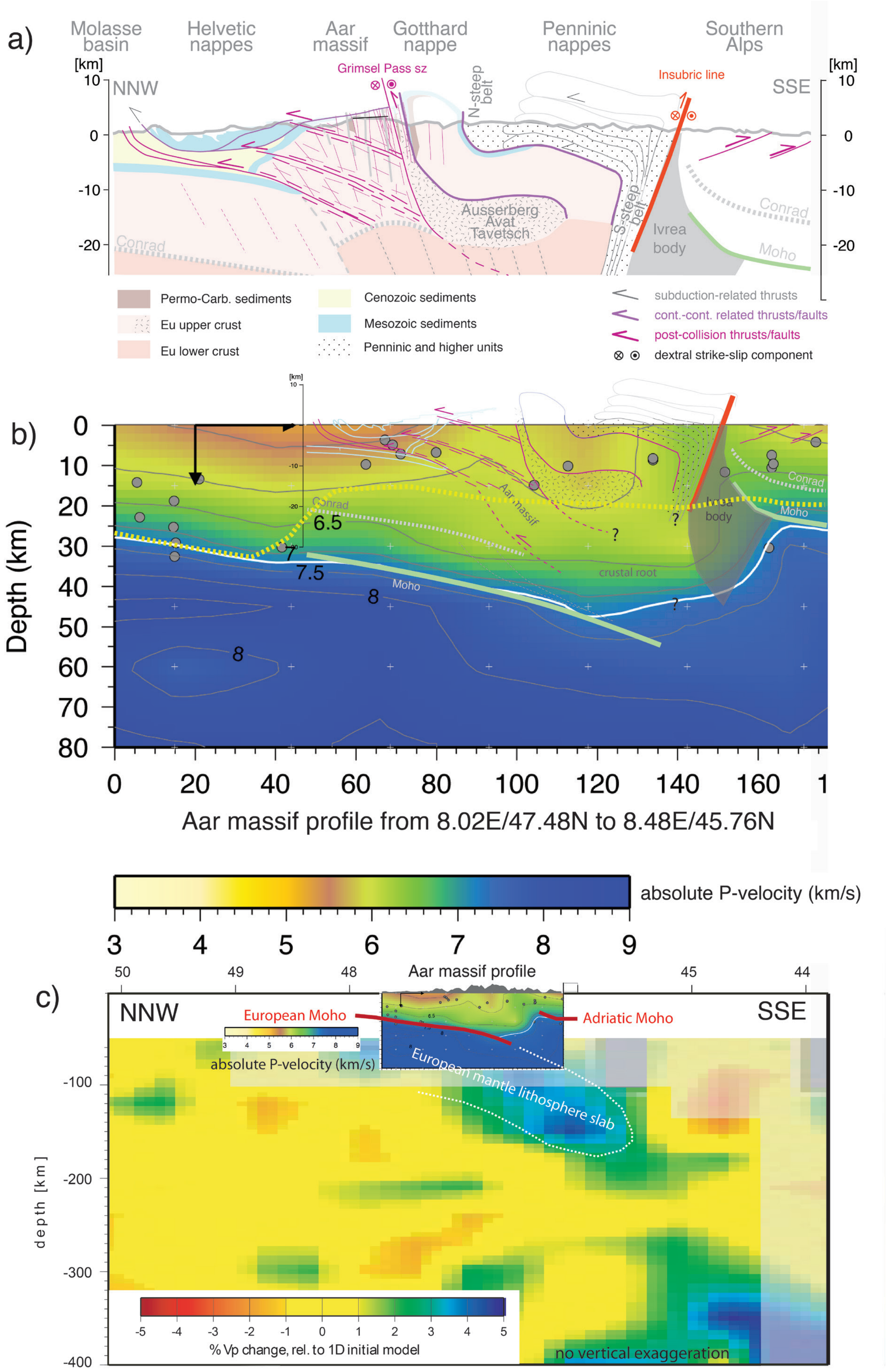

Fig. 2-14: (a) Crustal-scale cross-section through the central Alps (Aar Massiv), (b) vp seismic tomography and (c) teleseismic tomography (see Herwegh et al. 2017 for details).

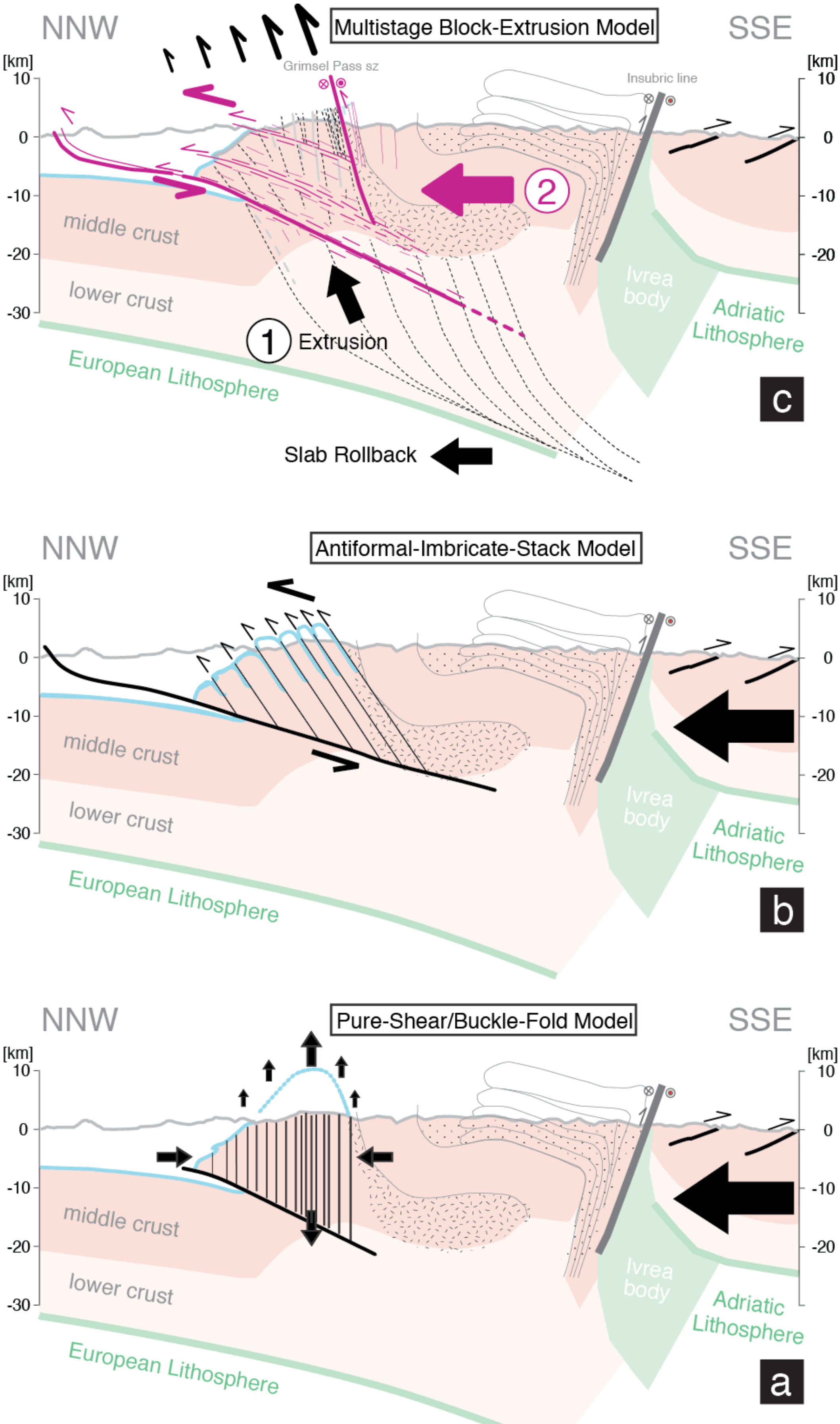

Fig. 2-15: Kinematic models suggested in the past for the exhumation of the Aar Massiv (see Herwegh et al. 2020 for details).

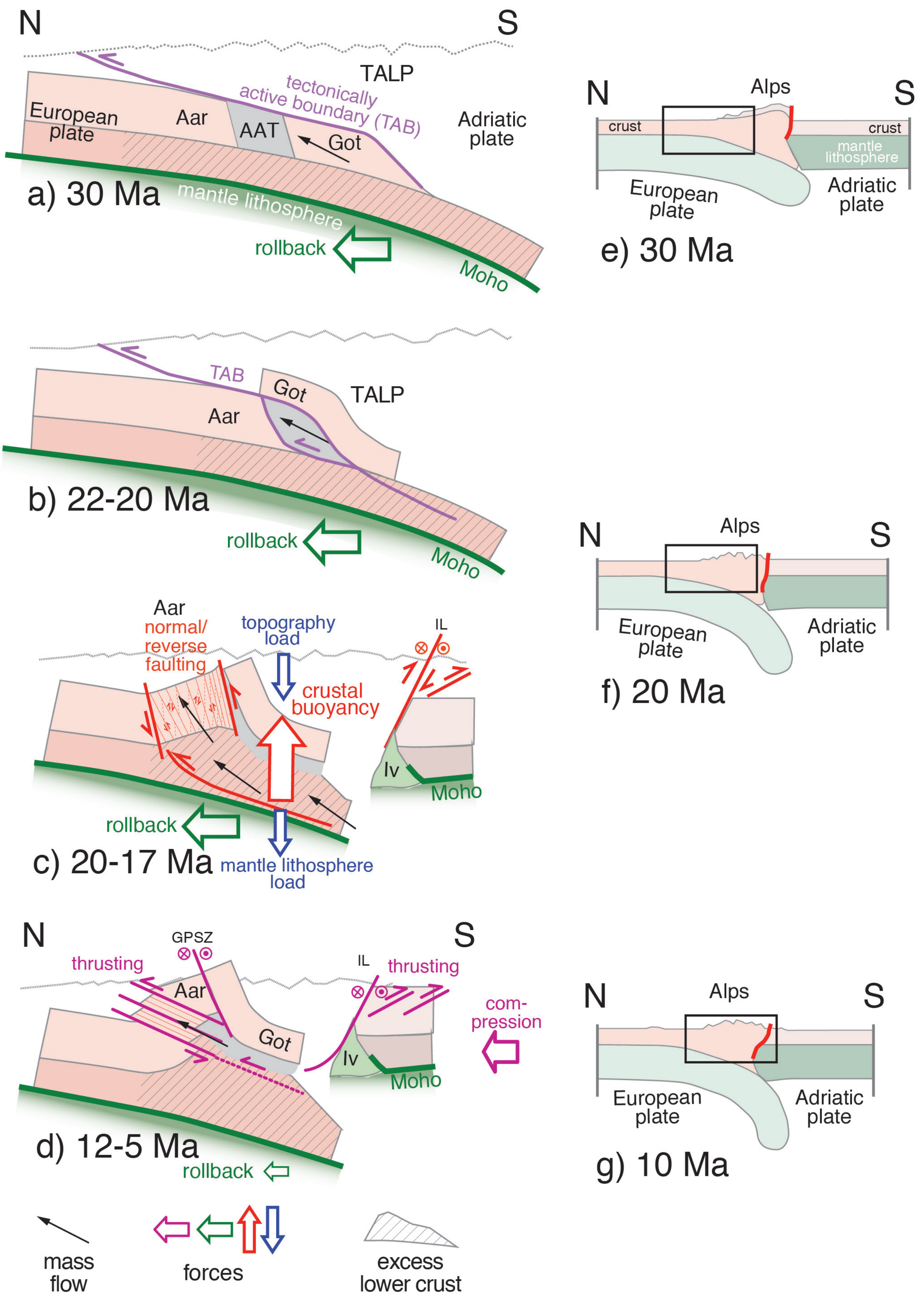

Fig. 2-16: Kinematic models suggested in the past for the exhumation of the Aar Massiv (see Herwegh et al. 2020 for details).

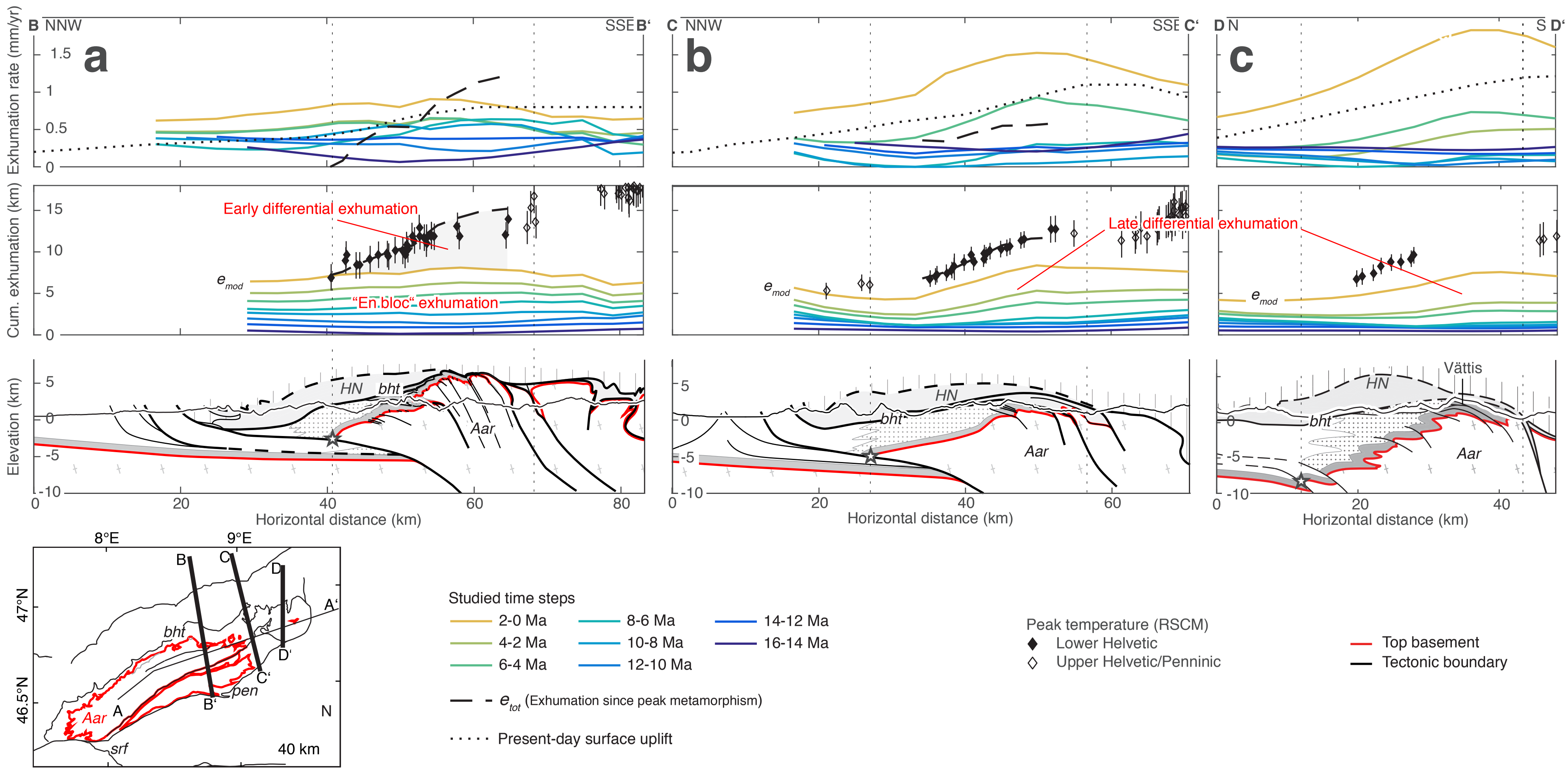

Fig. 2-26: Inverse model results plotted along (a) cross section B-B', (b) cross section C-C' and (c) cross section D-D'. See Fig. 2.21 for explanations. Legend and abbreviations as on Figure 1. The asterisks and the thin dotted black lines indicate the northern front of the Aar Massif. Present-day surface uplift rates are from Schlatter (2014).

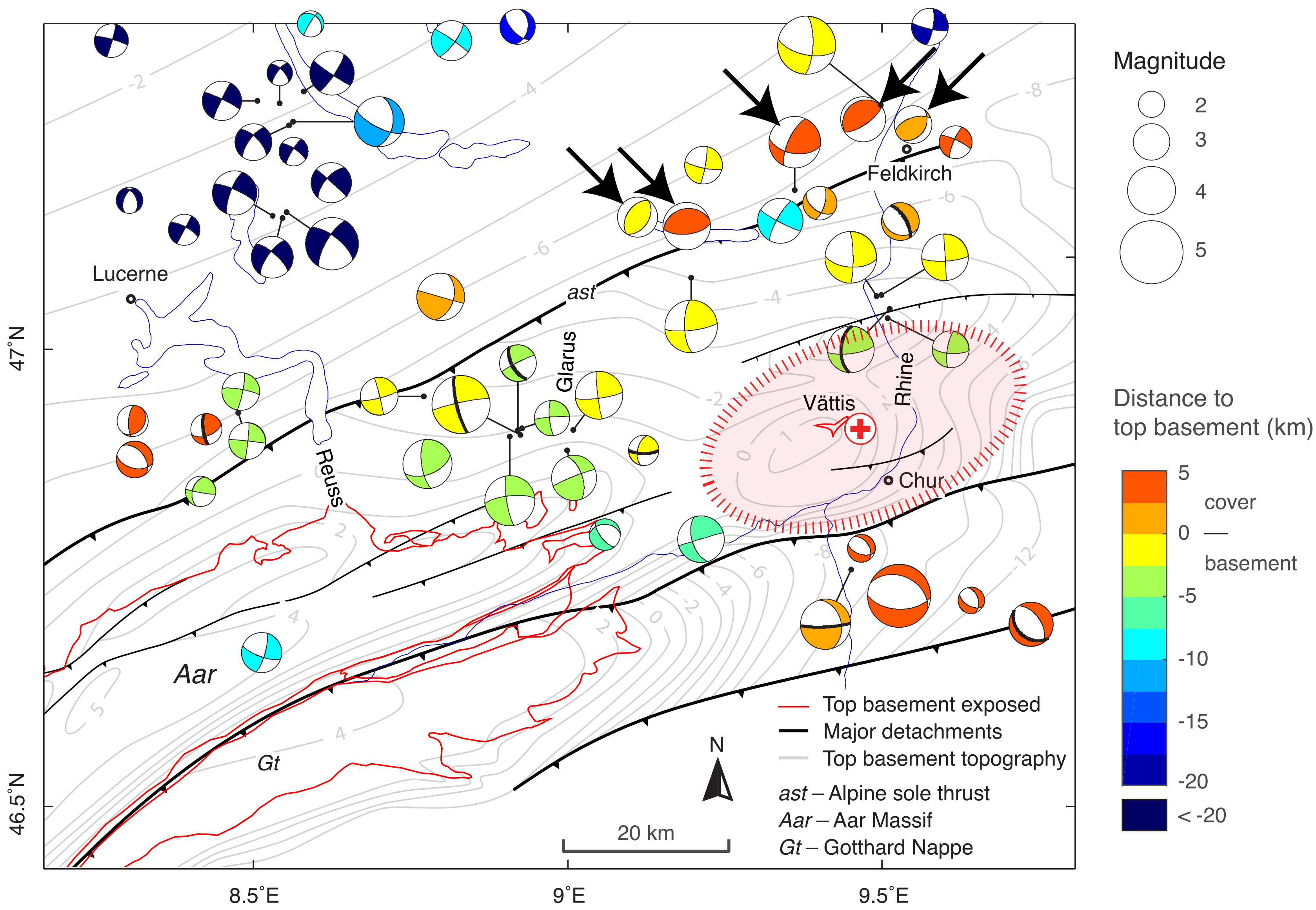

Fig. 2-28: Compiled earthquake focal mechanisms in the study area, coloured after distance to top basement for the years 1984 - 2018 (see text for references). Where identied, fault planes are highlighted as bold black lines. Top basement topography (shown as grey contour lines in the background) including major detachments (at the level of top basement) are from Pner (2011). The Aar Massif exposure is outlined by a solid red line. Black arrows highlight thrust-related earthquakes north of the Vättis area, the region of maximum post-2 Ma exhumation rates (red ellipse with dashed outline).

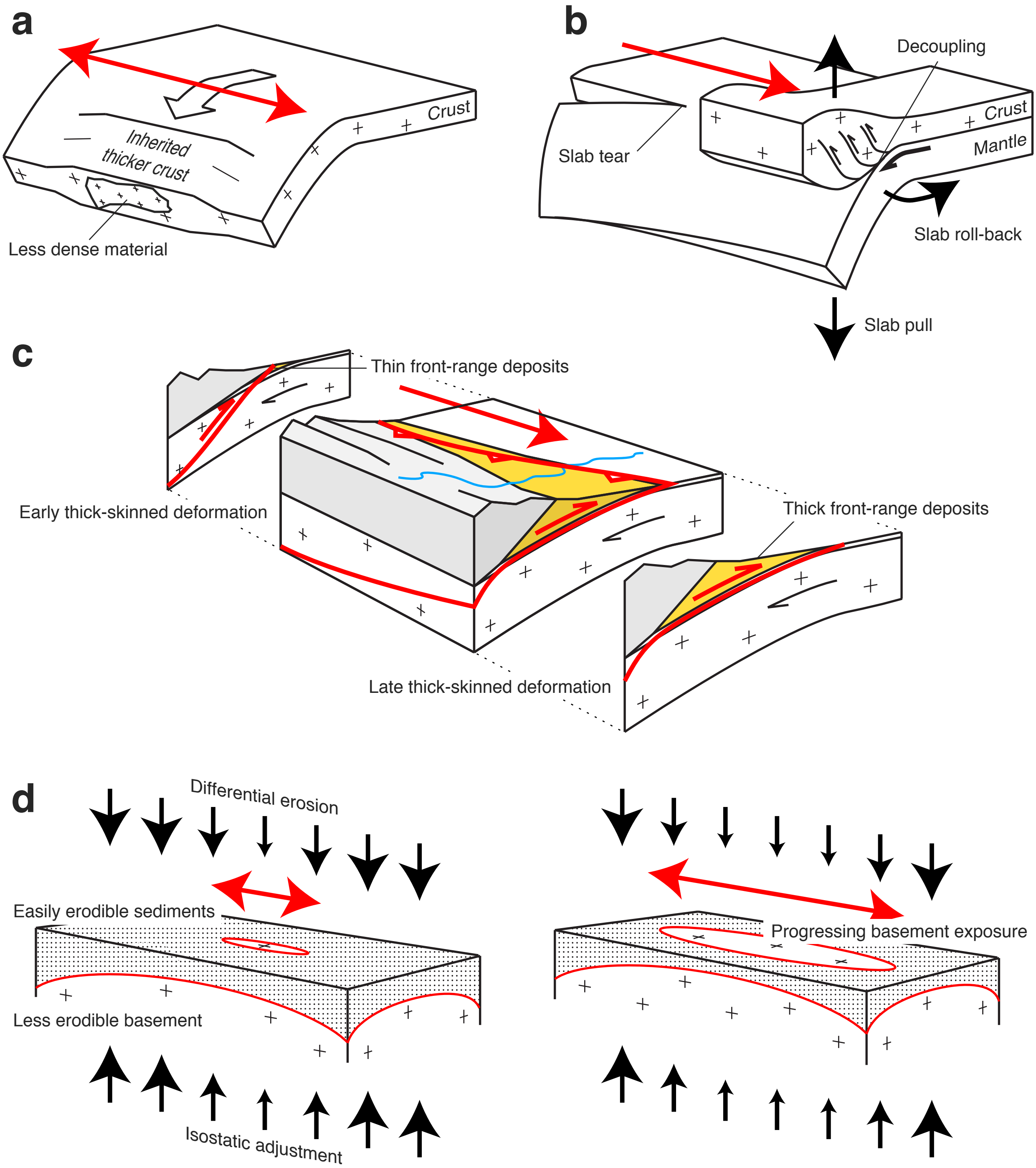

Fig. 2-29: Potential mechanisms to explain lateral changes in the exhumation dynamics.